DÉBORA GONÇALVES GOUVEIA

GROWTH INHIBITION IN AN *ARABIDOPSIS L,L*-DIAMINOPIMELATE AMINOTRANSFERASE MUTANT IS ASSOCIATED WITH BOTH METABOLIC IMPAIRMENTS AND GIBBERELLIN DEFICIENCY

Dissertação apresentada à Universidade Federal de Viçosa, como parte das exigências do Programa de Pós-Graduação em Fisiologia Vegetal, para obtenção do título de *Magister Scientiae.*

Orientador: Wagner Luiz Araújo

VIÇOSA – MINAS GERAIS
2021

Ficha catalográfica elaborada pela Biblioteca Central da Universidade Federal de Viçosa - Campus Viçosa

T
G719g
2021

Gouveia, Débora Gonçalves, 1990-
Growth inhibition in an *L,L*-diaminopimelate aminotransferase mutant is associated with both metabolic impairments and gibberellin deficiency / Débora Gonçalves Gouveia. – Viçosa, MG, 2021.
1 dissertação eletrônica (60 f.): il. (algumas color.).

Texto em inglês.
Orientador: Wagner Luiz Araújo.
Dissertação (mestrado) - Universidade Federal de Viçosa, Departamento de Biologia Vegetal, 2021.
Referências bibliográficas: f. 51-58.
DOI: https://doi.org/10.47328/ufvbbt.2021.152
Modo de acesso: World Wide Web.

1. *Arabidopsis*. 2. Aminoácidos. 3. Lisina - Metabolismo. 4. Giberelinas. 5. Inibidores enzimáticos. I. Araújo, Wagner Luiz. II. Universidade Federal de Viçosa. Departamento de Biologia Vegetal. Programa de Pós-Graduação em Fisiologia Vegetal. III. Título.

CDD 22. ed. 583.64

Bibliotecário(a) responsável: Alice Regina Pinto CRB6 2523

DÉBORA GONÇALVES GOUVEIA

GROWTH INHIBITION IN AN *ARABIDOPSIS L,L*-DIAMINOPIMELATE AMINOTRANSFERASE MUTANT IS ASSOCIATED WITH BOTH METABOLIC IMPAIRMENTS AND GIBBERELLIN DEFICIENCY

Dissertação apresentada à Universidade Federal de Viçosa, como parte das exigências do Programa de Pós-Graduação em Fisiologia Vegetal, para obtenção do título de *Magister Scientiae.*

APROVADA: 27 de julho de 2021.

Assentimento:

Débora Gonçalves Gouveia
Autora

Wagner L. Araújo
Orientador

AGRADECIMENTOS

Agradeço a Deus, por me fortificar a cada novo desafio e me dar a resiliência necessária para chegar até aqui e ir além.

Aos meus pais, Dorcas e Manoel, pela base, amor incondicional e confiança depositada, me fortalecendo dia-a-dia com inúmeras palavras de afeto.

Ao meu esposo e melhor amigo Wesley, por toda doçura e paciência. Sua confiança inabalável me fez acreditar que tudo seria possível.

À minha filha Laura, luz da minha vida. Que me faz enxergar que devo procurar todos os dias, a melhor versão de mim.

Ao meu orientador Professor Wagner L. Araújo, por toda paciência e otimismo. Agradeço-o pela confiança, disposição em ensinar, e comprometimento com meu crescimento profissional.

Ao Professor Adriano Nunes Nesi, pelos preciosos conselhos, ensinamentos compartilhados e disponibilidade em participar da banca de defesa.

Ao Professor João Henrique Cavalcanti, por toda a ajuda e incentivo, conversas esclarecedoras e disponibilidade em participar da banca de defesa.

Ao Professor Dimas Mendes Ribeiro, pela cordialidade e disponibilidade em participar da banca de defesa, além das valiosas contribuições neste trabalho.

Aos integrantes da Unidade de Crescimento de Plantas por terem me recebido com carinho, em especial à Dora, Marcelo, Jéssica, Paula e João Antônio por toda atenção, insights e apoio experimental.

Aos meus amigos de pós-graduação, que me deram o suporte emocional necessário para este processo, especialmente Hellen, Jailson e Rafael.

Ao Conselho Nacional de Desenvolvimento Científico e Tecnológico (CNPq), pela concessão da bolsa de estudos.

À Fundação de Amparo à Pesquisa do Estado de Minas Gerais (FAPEMIG) pelo suporte financeiro necessário para o desenvolvimento desse projeto.

O presente trabalho foi realizado com apoio da Coordenação de Aperfeiçoamento de Pessoal de Nível Superior – Brasil (CAPES) – Código de Financiamento 001.

À Universidade Federal de Viçosa e ao Programa de Pós-Graduação em Fisiologia Vegetal, pela oportunidade de realização do mestrado e estrutura disponibilizada.

Por fim, a todos que de maneira direta ou indireta contribuíram para a realização deste trabalho, os meus sinceros agradecimentos.

RESUMO

GOUVEIA, Débora Gonçalves, M.Sc., Universidade Federal de Viçosa, julho de 2021. **A inibição de crescimento no mutante *L,L*-diaminopimelato aminotransferase de *Arabidopsis* está associada tanto a deficiências metabólicas quanto à deficiência de giberelina.** Orientador: Wagner L. Araújo.

O metabolismo de lisina tem sido estudado a quase 40 anos sendo claramente envolvido na resposta de plantas a estresses, entretanto, questionamentos relativos à importância da lisina permanecem ainda em aberto. Aqui, investigaram-se os impactos metabólicos e fisiológicos da aplicação exógena de ácido giberélico (GA_3) sobre o desenvolvimento do mutante com atividade drasticamente reduzida da enzima de biossíntese de lisina *L,L*-DAPAT (*L,L*-diaminopimelate aminotransferase). A mutação DAPAT culminou no crescimento reduzido ao impactar o metabolismo do carbono e nitrogênio, provavelmente associado ao aparente estresse putativo, mesmo sob condições ótimas de crescimento. Em geral, a deficiência na síntese de lisina resultou em um menor teor de açúcares redutores e amido, especialmente ao final da noite. Além disso, um aumento substancial nos níveis de aminoácidos foi observado nas plantas mutantes *dapat*, indicando um ajuste metabólico e consequente desequilíbrio nos metabolismos de carbono e nitrogênio, possivelmente associado a continuidade do crescimento nas plantas deficientes na biossíntese de lisina. Plantas mutantes exibiram uma expressão diferencial dos genes *CPS*, *KS* e *GA3ox*, envolvidos na biossíntese de Giberelinas (GA). Notavelmente, a mutação DAPAT não eliminou a capacidade de resposta a aplicação exógena de GA deste mutante, promovendo a recuperação parcial do fenótipo anão característico. Embora o tratamento com GA_3 não pareça afetar o padrão metabólico das plantas mutantes, possivelmente é responsável pelo desequilíbrio C/N, evidenciado pelo incremento da expressão do gene marcador de sugar-starvation *DIN6*. Em conjunto, os resultados obtidos indicam que o metabolismo de lisina é um ponto-chave no balanço e alocação de carboidratos solúveis e de reserva, além de evidenciar a importância de *L,L*-DAPAT no controle do crescimento, metabolismo primário e da regulação hormonal.

Palavras-chave: Aminoácidos. Biossíntese de lisina. *L,L*-diaminopimelate aminotransferase. Giberelina. Reprogramação metabólica.

ABSTRACT

GOUVEIA, Débora Gonçalves, M.Sc., Universidade Federal de Viçosa, July, 2021. **Growth inhibition in an *Arabidopsis L,L*-diaminopimelate aminotransferase mutant is associated with both metabolic impairments and gibberellin deficiency.** Adviser: Wagner L. Araújo.

Lysine metabolism has been studied for almost 40 years and is clearly involved in plant response to stresses; however, questions regarding the importance of lysine remain open. Here, we investigated the metabolic and physiological impacts of exogenous application of gibberellic acid (GA_3) on the development of a mutant with drastically reduced activity of the lysine biosynthesis enzyme *L,L*-DAPAT (*L,L*-diaminopimelate aminotransferase). The DAPAT mutation culminated in reduced growth by impacting carbon and nitrogen metabolism, likely associated with apparent putative stress, even under optimal growth conditions. In general, the deficiency in lysine synthesis resulted in a lower content of reducing sugars and starch, especially at the end of the night. Furthermore, a substantial increase in amino acid levels was observed in *dapat* mutant plants, indicating a metabolic adjustment and consequent imbalance in carbon and nitrogen metabolisms, possibly associated with continued growth in plants deficient in lysine biosynthesis. Mutant plants exhibited a differential expression of *CPS, KS,* and *GA3ox* genes, involved in the biosynthesis of Gibberellins (GA). Notably, the DAPAT mutation did not eliminate the responsiveness to exogenous GA application of this mutant, promoting partial recovery of the characteristic dwarf phenotype. Although GA_3 treatment does not seem to affect the metabolic pattern of the mutant plants, it is possibly responsible for the C/N imbalance, evidenced by the increased expression of the sugar-starvation marker gene *DIN6*. Taken together, the results obtained indicate that lysine metabolism is a key point in the balance and allocation of soluble and reserve carbohydrates, and highlight the importance of *L,L*-DAPAT in controlling growth, primary metabolism, and hormone regulation.

Keywords: Amino acids. Lysine biosynthesis. *L,L*-diaminopimelate aminotransferase. Gibberellin. Metabolic reprogramming.

LISTA DE FIGURAS

SUMMARY

1. INTRODUCTION

Due to their sessile nature, plants need to constantly adapt to the fluctuating environment that surrounds them, with responses that involve dynamic changes in growth and signaling (GOLLDACK et al., 2013). Plant growth and development are tightly controlled by a range of intrinsic components that modulate morphological and physiological traits (HERNÁNDEZ-GARCÍA; BRIONES-MORENO; BLÁZQUEZ, 2020). Among these components, plant hormones not only modulate responses to the environment but also have an extensive impact on growth-related events (LJUNG; NEMHAUSER; PERATA, 2015; PAPARELLI et al., 2013).

Gibberellins (GAs), a large family of plant-specific hormones, play key roles in almost all aspects of the life cycle (HERNÁNDEZ-GARCÍA; BRIONES-MORENO; BLÁZQUEZ, 2020). GAs act in several developmental processes including seed germination, stem elongation, leaf expansion, root apical meristem growth, modulation of flowering time, and development of flowers and fruits (HAUVERMALE; ARIIZUMI; STEBER, 2012; OLSZEWSKI; SUN; GUBLER, 2002; RICHARDS et al., 2001; UEGUCHI-TANAKA et al., 2007). Since the identification of the first GA from higher plants, more than 130 GAs have been characterized. However, only a few of them are known to have biological activity, while non-bioactive GAs are either precursors of bioactive GAs or inactive forms (YAMAGUCHI, 2008). GAs are synthesized from geranylgeranyl diphosphate (GGPP) via a multistep pathway comprised of three major stages that correspond to the enzymes involved and their locations (HEDDEN, 2016; HEDDEN; KAMIYA, 1997). Briefly, the first step of GA synthesis occurs in the plastid with the cyclization of GGPP on *ent*-kaurene, in a two-step cyclization reaction and catalyzed by *ent*-copalyl diphosphate synthase (CPS) and *ent*-kaurene synthase (KS). Next, in the exterior of the endoplasmatic reticulum, mono-oxygenases dependent on cytochrome-P450, *ent*-kaurene oxidase (KO), and *ent*-kaurenoic acid oxidase (KAO) generate GA_{12} that can be further converted to GA_{53}. Last but not least, in the cytosol, GA_{12} and GA_{53} are converted to different GA intermediates and bioactive forms through consecutive oxidations performed by GA3-oxidase (GA3ox),

GA20-oxidase (GA20ox), and 2-oxoglutarate-dependent dioxygenases (OLSZEWSKI; SUN; GUBLER, 2002).

There is compelling evidence suggesting that the metabolism of hormones is associated with plant growth (e.g GAs), is directly affected by the availability of carbohydrates, and thus indicating that plant growth may be coordinated with the availability of adequate carbon levels (PAPARELLI et al., 2013). The significance of GAs in plant growth modulation is derived from several independent analyses by using inhibitors of GA biosynthesis (RIBEIRO et al., 2012; TANIMOTO, 1988) or GA deficient mutants in different plant species. Briefly, GA deficient mutants are usually characterized by a dwarf phenotype as well as a germination deficiency and typically exhibit delayed flowering and reduced fertility (MARTINS et al., 2019; RICHARDS et al., 2001; SUN, 2008).

Paclobutrazol (PAC), a GAs biosynthesis inhibitor, affects seed germination, plant growth, and GA content (RADEMACHER, 2000), in addition to promoting opposed behavior between shoot and root systems (BIDADI et al., 2010; MARTINS et al., 2019; RIBEIRO et al., 2012). Remarkably, the observed growth retardation in PAC-treated plants also induced an exquisite metabolic adjustment in response to a low-GA regime, which strongly suggests the uncoupling between growth and carbon availability for these plants. Nevertheless, the phenotype caused by PAC can be completely reverted to the wild-type (WT) phenotype by exogenous application of gibberellic acid (GA_3)(RIBEIRO et al., 2012). Collectively, the aforementioned results led to a better understanding of the effects of GAs deprivation conditions on the integration of carbon metabolism and plant growth.

By acting in coordination with plant hormones, primary metabolism drives plant growth, where nutrient sensing and hormonal signaling are essential (LJUNG; NEMHAUSER; PERATA, 2015). Sugars formed during photosynthesis are dynamically split between growth, metabolic processes, and storage (PAPARELLI et al., 2013). Accordingly, during the night, energy and carbon intermediates are produced through the respiratory process that oxidizes organic acids via both the glycolysis and tricarboxylic acid (TCA) cycle. Thus, energy availability must be maintained to allow continuous growth

and the maintenance of cell metabolism throughout the diel cycle (NUNES-NESI et al., 2008; SMITH; STITT, 2007).

A transient sugar deficit may occur when energy availability is perturbed, leading to temporal interruption of plant growth (IZUMI et al., 2013). Notably, low energy stress is mimicked in mutants with impaired starch synthesis and/or degradation. Starchless mutants are smaller than WT plants, indicating that the lack of starch metabolism causes a carbon deficiency at night, directly affecting its growth (GIBON et al., 2004; STITT; ZEEMAN, 2012). PAPARELLI et al., (2013) demonstrated that *Arabidopsis* mutants defective in starch synthesis and breakdown induce nighttime sugar starvation, with a marked reduction in the expression of *ent*-kaurene synthase (*KS*), one key enzyme for GAs synthesis. Furthermore, starch defective mutants are usually characterized by growth impacts (GIBON et al., 2009; SULPICE et al., 2009) which are partially or completely restored by exogenous GA_{4+7} treatment (PAPARELLI et al., 2013).

Sugar availability is fundamental for plants to cope with their changing day/night periods and environmental variations (SMITH; STITT, 2007). Briefly, plants must reprogram their metabolism to synthesize alternative respiratory substrates to provide energy and maintain its growth, development, and mainly, its survival under these harsh conditions (ARAÚJO et al., 2011; IZUMI et al., 2013). Although plant respiration is primarily dependent on sugar oxidation, under stress conditions (which affect carbohydrates supply), the importance of protein and amino acids must not be underestimated. Under carbon starvation, especially during stress conditions, plant metabolism is rather altered and other pathways are induced to provide alternative substrates to sustain respiratory processes (ARAÚJO et al., 2011; BARROS et al., 2017; HILDEBRANDT et al., 2015; IZUMI et al., 2013).

In mammals, the electron-transfer flavoprotein: ubiquinone oxidoreductase (ETFQO), which is associated with the inner mitochondrial membrane, accepts electrons from the electron-transfer flavoprotein (ETF) localized in the mitochondrial matrix (BECKMANN; FRERMAN, 1985; RUZICKA; BEINERT, 1977). To date, only two alternative dehydrogenases, namely isovaleryl-CoA dehydrogenase (IVDH) and *D*-2 hydroxyglu-

tarate dehydrogenase (D2HGDH), have been demonstrated to be able to donate electrons to the ETF/ETFQO system in plants (ARAUJO et al., 2010; ENGQVIST et al., 2009). It has been previously demonstrated that products derived from the ETF/ETFQO pathway (lysine and the branched-chain amino acids – BCAA, isoleucine, leucine, and valine) represent alternative electron donors at the mitochondrial level (ARAUJO et al., 2010; ENGQVIST et al., 2009). This donation of electrons occurs either directly by the transfer of electrons to the mitochondrial electron transport chain (mETC) via ETF complex or indirectly by the direct feeding of catabolic products into the TCA cycle (ARAUJO et al., 2010). The identification and characterization of IVDH, D2HGDH, ETF, and ETFQO proteins, directly related to the catabolism of several amino acids, that are up-regulated mainly under stress conditions, reinforce an alternate electron supply to the mETC via ETF complex (ARAUJO et al., 2010; ISHIZAKI, 2005; ISHIZAKI et al., 2006).

Lysine is an essential amino acid that connects the amino acid metabolism to the mETC and TCA cycle, whose cellular concentration must be tightly adjusted by its synthesis and degradation (ARAUJO et al., 2010; AZEVEDO et al., 1997; CAVALCANTI et al., 2018; GALILI, 2011; KIRMA et al., 2012). In land plants, lysine is synthesized via a pathway starting with aspartic acid (Asp), which also leads to the formation of threonine (Thr), methionine (Met), and isoleucine (Ile) (Figure 1). Lysine synthesis has also been described for bacteria, fungi, and some protozoa although not all of these groups share the same metabolic pathways for amino acid synthesis (ARRUDA et al., 2000; HUDSON et al., 2005).

Bacteria use normally one (or more) of the three biosynthetic pathways of lysine, and the same mechanism was thought to be used by plants. Yet, land plants have an even more dynamic mechanism, which is the direct conversion of *L*-tetrahydrodipicolinic acid (*L*-THDP) to *L,L*-diaminopimelate (*L,L*-DAP) catalyzed by the enzyme *L,L*-DAP aminotransferase (*L,L*-DAPAT), which has a sequence identity equal to 20% concerning bacterial DAPATs (HUDSON et al., 2006; WATANABE et al., 2007). In comparison to bacteria, the activity of the plant DAPAT replaces three enzymatic steps in this pathway (HUDSON et al., 2006).

It has been demonstrated that a C-to-A point mutation in the DAPAT (AT4G33680) gene, that encodes the enzyme *L,L*-DAPAT in *Arabidopsis*, led to a dwarf phenotype, alteration of leaf morphology, and accumulation of salicylic acid (RATE; GREENBERG, 2001; SONG, 2004). This hypomorphic mutant presents a single amino acid substitution in the *L*,*L*-DAPAT that resulted not only in a marked reduction in enzyme activity but also led to metabolic shifts and growth inhibition (CAVALCANTI et al., 2018). The putative energy deprivation scenario observed in *dapat* mutant plants included a lower accumulation of starch at the end of the day (ED), and suggestive high protein degradation, implying that a C/N imbalance is most likely to support energy generation by alternative pathways of mitochondrial respiration, with an uncoupling growth from primary carbon metabolism. Consequently, *dapat* plants were proposed to present a marked metabolic phenotype that mimics stress responses, likely associated with impairments in the lysine biosynthesis pathway (CAVALCANTI et al., 2018).

Particularly in *A. thaliana*, lysine degradation occurs through a branched pathway (ARAUJO et al., 2010). The bifunctional enzyme lysine-ketoglutarate reductase (LKR)/saccharopine dehydrogenase (SDH) (LKR/SDH) converts lysine into saccharopine, later to 2-aminoadipic-6-semialdehyde. Glutamate is one of the products of lysine degradation by transamination, leading to the conclusion that lysine is converted in acetyl-CoA and subsequently to 2-OG by the TCA cycle (Figure 1). Remarkably, the discovery of the direct production of 2-OG in an alternative route catalyzed by the D-2-hydroxyglutarate dehydrogenase enzyme (D2HGDH) (ARAUJO et al., 2010; ENGQVIST et al., 2009), revealed a strong correlation between the TCA cycle and alternative respiration in the maintenance of energy metabolism (ARAUJO et al., 2010; GU; JONES; LAST, 2010; PIRES et al., 2016). Therefore, lysine catabolism either by D2HGDH or LKR/SDH reinforces the critical role of this amino acid as an auxiliary source of electrons carried by the ETF-ETFQO complex to support plant cell ATP production (ANGELOVICI et al., 2011).

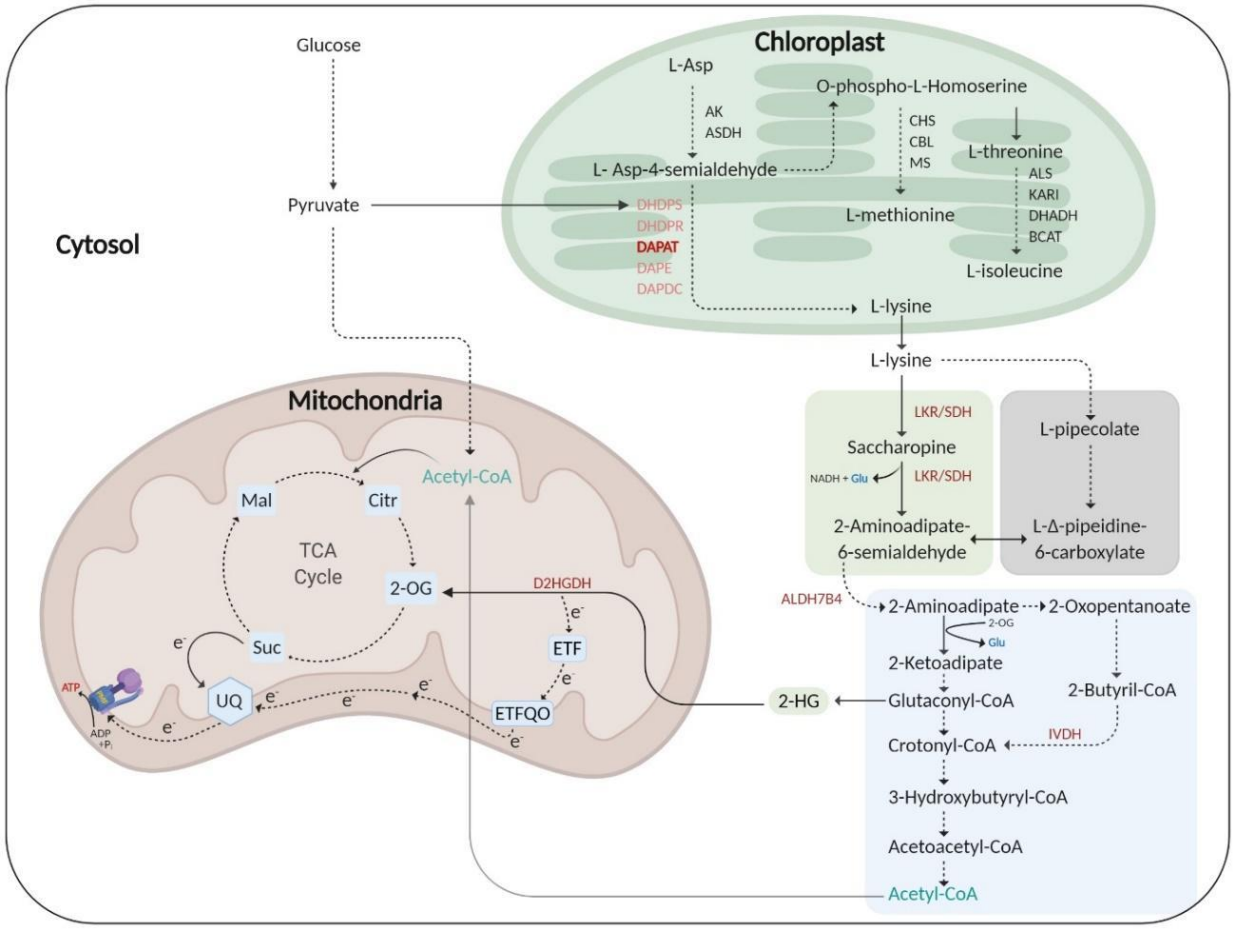

Figure 1 - Schematic representation of lysine metabolism in land plants.

Lysine is synthesized in the chloroplast through the aspartic acid (Asp) pathway, which is also responsible for the biosynthesis of threonine, methionine, and isoleucine. Lysine catabolism yields acetyl-CoA and/or 2-oxoglutarate (2-OG), and Glutamate is the transamination product. Under stress conditions, lysine is degraded by LKR/SDH or D2HGDH enzymes, donating electrons to the ETF-ETFQO complex, and simultaneously reinforcing cell ATP production. Individual reaction steps have been extensively characterized in plants (light green boxes). However, the major part of the lysine pathway catabolism (light blue box) requires further experimental evidence. Additionally, one alternative route for the reaction catalyzed by the bifunctional enzyme LKR/SDH (light green box) via the L-pipecolate is also indicated (gray box). Abbreviations: AK, Aspartate kinase; ASDH, Aspartate-semialdehyde dehydrogenase; DHDPS, Dihydrodipicolinate synthase; DHDPR, Dihydrodipicolinate reductase; *L,L*-DAPAT, *L,L*-

diaminopimelate aminotransferase; DAP, Diaminopimelate E; DAPDC, Diaminopimelate decarboxylase; ALS, Acetolactate synthase; KARI, Ketoacid reductoisomerase; DADH, Dihydroxyacid dehydratase; BCAT, Branched-chain aminotransferase; CHS, Chalcone synthase; LKR/SDH, Lysine-ketoglutarate reductase/saccharopine; ALDH7B4, Aldehyde dehydrogenase 7B4; IVDH, Isovaleryl-CoA-dehydrogenase; ETF/ETFQO, Electron transfer flavoprotein-ubiquinone oxidoreductase; D2HGDH, D2-hydroxyglutarate dehydrogenase; Ctr, Citrate; Mal, malate; Suc, Succinate; UQ, Ubiquinone.

Although growth inhibition that mimics stress conditions in *dapat* mutant plants was associated with extensive metabolic reprograming (CAVALCANTI et al., 2018), the specific molecular mechanism that triggers an energy limitation scenario in which DAPAT mutation is metabolically involved remains poorly characterized. In an attempt to better understand how and to which extent this connection occurs, as well as the importance of lysine biosynthesis in modulating plant growth responses, we used an *A. thaliana* lysine biosynthesis mutant (*dapat*), with reduced activity of the lysine biosynthesis enzyme *L,L*-DAPAT (CAVALCANTI et al., 2018; HUDSON et al., 2006).

Considering that uncoupling between carbon and nitrogen metabolism was observed in leaf tissues of plants with both alterations in the endogenous content of GAs (RIBEIRO et al., 2012a, 2012b) and the lysine biosynthesis (CAVALCANTI et al., 2018), we observed that growth impairments in the lysine deficient mutant plants are seemingly mitigated by exogenous GA. By further investigating the metabolic and physiological impacts of exogenous GA application on both the growth and development of *dapat* mutant plants, we demonstrated the metabolic adjustments that are triggered by the DAPAT mutation. The results obtained so far allow us to expand our current knowledge of the adjustments that are triggered by the impaired biosynthesis of lysine, in addition to clarifying, at least partially, how this deficiency can impact the acclimatization of plants and their response to energy stress.

2. OBJECTIVES

The main goals of this research initiative were (*i*) to evaluate the metabolic and physiologic significance of exogenous GA treatment on the primary metabolism of *dapat* plants, (*ii*) to enhance our understanding of the role of lysine during stress responses, and (iii) to characterize the connections between lysine and GA metabolism in *Arabidopsis thaliana* by using a lysine biosynthesis deficient mutant.

To reach these aims, the planned research was organized around three main tasks:

1. Growth analysis of *dapat* mutant plants in response to GA.

2. Metabolic and physiological characterization of *dapat* mutants under exogenous GA application.

3. Expression analysis of genes involved in GA and amino acid metabolism to elucidate how lysine modulate the how lysine modulate stress response in plants

3. MATERIALS AND METHODS

3.1. Plant material and growth conditions

Arabidopsis thaliana wild-type (WT) and the lysine biosynthesis mutant *dapat* [previously referred to as *aberrant growth death 2* (*agd2*) characterized by (RATE; GREENBERG, 2001)], both of Columbia-0 ecotype (Col-0), were used. Seeds were surface sterilized in 1 mL of 70% ethanol for two minutes with manual shaking. After the ethanol was removed and 1 mL of 1.25% sodium hypochlorite was added for 15 minutes, with constant stirring. The entire sodium hypochlorite residue was removed by repeated washing (6x) in 1 mL autoclaved deionized (reverse osmosis) water (DIW). After the sterilization process, the seeds were imbibed for 4 days at 4°C in 1 mL of autoclaved DIW in the dark. Immediately after, the seeds were put to germinate on 0.7% (*w/v*) agar plates containing half-strength MS media (pH 5.7) (MURASHIGE; SKOOG, 1962), supplemented with 1% sucrose.

Seeds were subsequently germinated and grown under short-day conditions (8 h light/16 h dark), at 20ºC and 60% relative humidity. Afterward, 10-day-old seedlings were

transferred to individual 0.08 dm^3 pots containing commercial substrate Carolina Soil Standard (EC 0.7 - 8 Kg) and kept in the same growth conditions for 3 weeks.

3.2. PCR - Restriction Fragment Length Polymorphism (PCR - RFLP)

The missense mutation caused by the mutagenic ethyl methanesulfonate (EMS) in *dapat* plants promotes the loss of a *Hha*I restriction and due to the shift to this restriction endonuclease (RN) recognition site, genotyping was possible by PCR-RFLP.

Firstly, genomic DNA was extracted from seeds (DELLAPORTA; WOOD; HICKS, 1983), and was evaluated in 1% agarose TAE 1X gel with a Mid-Range DNA ladder (Cellco Biotec MMK-108S) and by spectrophotometry for quality control. Subsequently, gDNAs were amplified with selected primers (AGD2_HhaI_FW and AGD2_HhaI_RV primers - Table 1) flanking a 1219 bp region (chromosome 4, from 16311616 to 16312834).

Table 1 – Genotyping primers flanking a 1219 bp region *Arabidopsis* DNA comprising the AGD2-1 gene.

Primers	Sequence	Tm (ºC)	*Hha*I digestion Fragments
AGD2_HhaI_ FW	TTCTCAGACAG-TGTTCCTCC	56.50	WT: 647 bp, 263 bp, 233 bp, and 76 bp
AGD2_HhaI_ RV	CTGCACTT-GTTTCAATGGTGC	58.87	*dapat:* 910 bp, 233 bp, and 76 bp

* PCR Cycling: 94ºC for 30''; 40 cycles of 94ºC for 30''; 50ºC for 30''; 72ºC for 1'10''. The final step was 72ºC for 5'

The PCRs followed the parameters presented in Table 1, and the resulting amplicons were checked through 1% agarose TAE 1X gel with a Mid-Range DNA ladder (Cellco Biotec MMK-108S) (MRL). Amplicons were purified using the Wizard® SV Gel and PCR Clean-Up System (Catalog number: A9281) and evaluated in a 1% agarose TAE 1X gel and by spectrophotometry. Purified amplicons harbor 3 *Hha*I recognition sites in the WT and only 2 recognition sites in the *dapat* mutant, therefore, the *Hha*I digestion yields different patterns as shown in Table 1.

Invitrogen™ Anza™ 59 *Hha*I (Catalog number: IVGN0596) RN was used to digest the purified amplicons following the manufacturer's protocol. To this end, 900 ng of each

amplicon were incubated for 1 h at 37 ºC in a dry bath, then, digested products were loaded in a 1.5% agarose TAE 1X gel for 80 min at 80 V (fixed) and 400 mAh with MRL to verify the digestion patterns for WT and *dapat* plants.

3.3. GA treatment application

Three-week-old plants were grown exactly as described in 3.1 at a PPFD of 150 µmol photons m^{-2} s^{-1} and submitted to five applications of 20 µL of 25 mM Gibberellic acid (Sigma-Aldrich G7645) for 14 days, with an interval of 72 hours per application. During the experiment, WT and *dapat* mutant plants were photographed at each application for the evaluation of visual phenotypes. At the end of this period, shoot samples were collected, immediately frozen in liquid nitrogen, and stored at -80 ºC until further analyses.

3.4. Biometric Parameters

Whole rosettes of 5-week-old plants were collected and the rosette fresh weight (RFW), rosette dry weight (RDW), total rosette area (TRA), total leaf area (TLA), specific leaf area (SLA), and the number of rosette leaves (NL) were determined. The SLA was estimated using the following formula:

$$SLA = TLA / RDW$$

The images obtained were further processed using the Image J® software version 1.5.2 (SCHNEIDER; RASBAND; ELICEIRI, 2012).

3.5. Leaf gas exchange parameters

Gas exchange and chlorophyll *a* fluorescence analyses were performed simultaneously using an open-flow infrared gas exchange analyzer system equipped with an integrated fluorescence chamber (IRGA, LI-COR Inc. LI-6400XT; NE). Instantaneous gas exchanges, including net CO_2 assimilation rate of carbon (A), stomatal conductance (g_s), and the internal carbon dioxide concentration (C_i) were analyzed in 5-week-old plants, which were acclimatized for 1 hour after the start of the light period. The reference CO_2 concentration was set at 400 µmol CO_2 mol^{-1} air and gas exchange was determined under

1000 µmol photons m^{-2} s^{-1}. The IRGA chamber was maintained at 25 ºC and the leaf-to-air vapor pressure deficit kept between 1.0-1.5 kPa, with all measurements were performed using the 1 cm^2 leaf chamber. Dark respiration (R_d) was determined using the same gas exchange system described above after at least 2h after the start of the dark period (at night) using the same leaf previously used to determine *A*.

3.6. Determination of Metabolite Levels

Leaves of the whole rosette were harvested two hours before the end of the light (end of the day; ED) or dark (end of the night; EN) period. The harvest time was based on the expression pattern of the *ent-kaurene synthase* (*KS*) gene, which peaks in the afternoon of the diurnal cycle (PAPARELLI et al., 2013).

Methanolic extraction was performed by rapid grinding approximately 25mg of fresh leaf mass with liquid nitrogen and the immediate addition of the appropriate extraction buffer. The chlorophyll contents (*a* and *b*) were determined as previously described (PORRA; THOMPSON; KRIEDEMANN, 1989). The determination of starch (FERNIE, 2001) and total protein levels (BRADFORD, 1976) was performed with the insoluble fraction. In the soluble fraction, the contents of organic acids (NUNES-NESI et al., 2007), glucose, fructose, and sucrose (FERNIE, 2001), and total soluble amino acids (GIBON et al., 2004) were measured.

3.7. Gene expression analysis

The expression of the main representative genes involved in GA metabolism, metabolism of amino acids, and the activation of alternative respiration pathways was analyzed with reverse quantitative transcription-PCR (RT-qPCR - Table 2) by the relative-expression method.

Total RNA was extracted from the samples with TRIzol reagent (Ambion, Life Technology). After purification, the RNA was quantified by NanoDrop ND-2000 spectrophotometer (Thermo Scientific NanoDrop Technologies, Wilmington, Delaware, United States) and analyzed on a 1,5 % (w/v) agarose gel. A total of 0.5 µg of RNA was treated

with DNAse I (Invitrogen®) to remove potential contamination with genomic DNA. The cDNA synthesis was performed using 0.5 µg of total RNA using GoScript™ Reverse Transcriptase (A5003) + RNasin Ribonuclease Inhibitor + master mix with Oligo(dT) (A2791) following manufacturer protocol. For the analysis of gene expression, Ludwig qPCR-SYBR-Green mix/ROX (ID:40) was used following the manufacturer protocol with the MicroAmpTM Optical 96-well Reaction Plate (Applied Biosystems, Singapore, China) and MicroAmpTM Optical Adhesive Film (Applied Biosystems, Foster City, CA, USA).

The relative expression levels were normalized using the housekeeping gene *EF1a* (WANG et al., 2014). The primers used for RT-qPCR were designed using the Primer3Plus web application (UNTERGASSER et al., 2012). The independent genotypes were represented by at least three plants and the mean value of the expression was calculated by the relative-expression method and represented as the normalized $2^{-(\Delta Ct)}$ with its respective standard errors. The normalizer was set as the average of three WT $2^{-(\Delta Ct)}$ values of each gene, then, the relative-expression was calculated as the average of three values of normalized $2^{-(\Delta Ct)}$ of each group analyzed. The results were analyzed using the Tukey test at the 5% level.

Table 2 – Selected genes and primers used for expression analysis in *dapat* mutant plants submitted to GA treatment.

Gene	Locus	Pathway	Forward Primer	Reverse Primer
AGD2	AT4G33680	Lysine biosynthesis	CTGGAGAAGACTCATGTG	AGATGTTCTCTCTGTGACC
LKR/SDH	AT4G33150	Lysine catabolism	TGATTGTCGCGTCTCTGTATC	ATCTAGCCGAACTGCTTCTAC
D2HGDH	AT4G36400	Lysine catabolism	GAAGCTGTCATATCGGTGGA	TCGTACCCAGTATTGTCTTTGC
IVDH	AT3G45300	BCAA catabolism	AATGGGAAAGTTGACCCAAAGGAC	TAAAGCGACCTGCGTTGCTCTC
ETFQO	AT2G43400	Alternative respiration	TTGGCCATTAGTGCTATGGAACAC	TCCCATGCTTGAGCGTGAAAGG
CPS	AT4G02780	GAs metabolism	CTCAATGTCGCTAGAGAC	GTTGCCACTCATGTATTAG
KO	AT5G25900	GAs metabolism	ATGTCTGAAGTCTCCACTC	AGGACCATAAATCTCTGAC
KS	AT1G79460	GAs metabolism	GGTGGAGTACTTACAACG	CATGTTCTGAGCTGTACTC
GA3ox1	AT1G15550	GAs metabolism	AGACGATCTCCTCTTCTC	AGTTCTACATGCATGACC
GA20ox1	AT4G25420	GAs metabolism	CGGGACTACTTTAGAGAG	TCCTGTTCCTAGTGTGAG
DIN6	AT3G47340	Sugar-starvation marker	TGGCTTGTTCGACTGCAAAG	AATGCCACGTTCTTGCCATC
ATL8	AT1G76410	Sugar-starvation marker	TGCGGTTCTTCTTTGTGCAC	CTTTGTTGGCTGCAGCTACC
EF1a	AT5G60390	Constitutive Gene - Elongation Factor 1 alfa	CACGAGTCTCTTCTTGAG	TCATCCTTGGAGTTAGAG

3.8. Protein-protein interaction network analyses

A functional network of proteins was predicted using STRING version 11.5 (SZKLARCZYK et al., 2021), available at www.string-db.org. Functional protein-association networks were visualized with high confidence (0.7), with *A. thaliana* data set.

3.9. Statistical Analyses

All experiments were performed in a completely randomized experimental design (CRD). Statistical analyses were performed using the statistical software RStudio version 1.4.1106 (RStudio Team, 2020). All data are expressed as the mean ± standard error (SE) of five independent replicates per genotype, and when was the case, over time. The averages of the treatments were compared by Tukey's test ($P \leq 0.05$).

4. RESULTS

4.1. Confirmation of the *LL*-DAPAT mutation

To investigate the *in vivo* function of lysine biosynthesis deficiency an *Arabidopsis* mutant with a single mutation in the *L,L*-DAPAT was used (Figure 2). The *dapat* mutant was generated via a single nucleotide polymorphism through EMS mutation (from G to A) in the DAPAT gene that encodes for one of the lysine biosynthesis enzymes in plants, the *L,L*-DAPAT. The mutation causes a missense in the encoded enzyme due to the substitution of the amino acid proline for one serine at position 398 (Figure 2), leading to a loss of about 90% of the enzyme activity (CAVALCANTI et al., 2018; HUDSON et al., 2006).

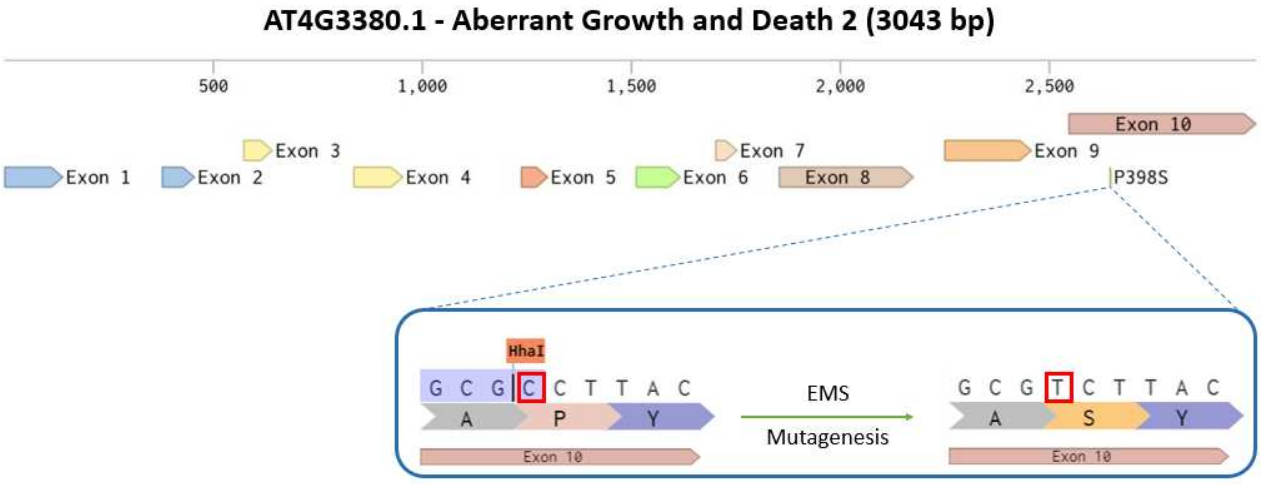

Figure 2 - Overview of the mutation localization in the DAPAT gene.

Schematic diagram showing the chemical mutation in the DAPAT gene (AT4G33680). The red square indicates the Pro-to-Ser change caused by the agd2 allele. In plants, this mutation leads to dwarfism, altered leaf morphology, and enhanced accumulation of salicylic acid (SA), and was therefore originally named the '*Aberrant Growth and Death*' (*agd2*) mutant (RATE; GREENBERG, 2001) PCR-RFLP genotyping of *dapat* and wild-type (WT).

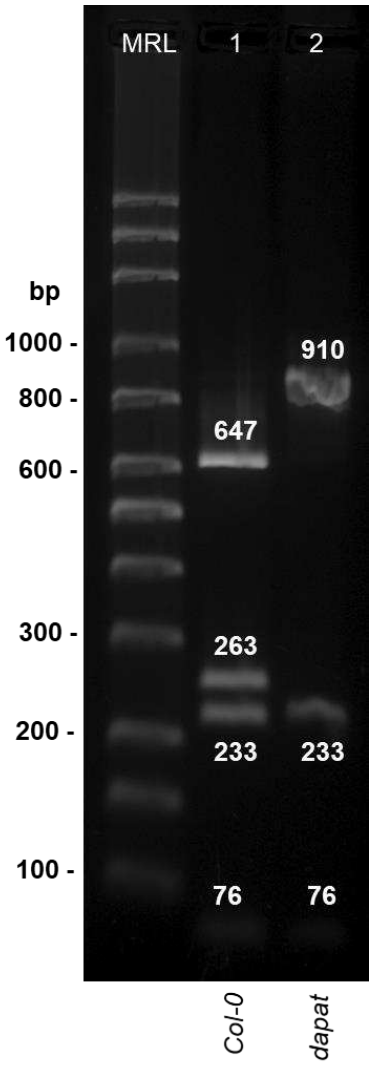

Figure 3 - ***dapat* genotype was confirmed based on the shift in the restriction pattern due to the G to A SNP in *dapat* seeds.**

Genotyping was performed with total DNA from seeds of the wild-type (WT; Col-0) and the *dapat* mutant by PCR-RFLP in 1,5% agarose TAE 1X gel**.** The first column was loaded with 3 µL of MRL, sample 1 represent WT *Hha*I digested amplicon and sample 2 represent *dapat Hha*I digested amplicon. For both samples, 10 µL of digested amplicon were loaded in each well.

Through PCR-RFLP analysis, it is possible to affirm that *dapat* and WT correspond to their genotypes by the characteristic *Hha*I digestion patterns shown by the seed material (Figure 3) and plant material (Figure 4). As expected, in WT a band of 647 bp near to 600 bp in the MRL was observed, whereas, in *dapat* mutant plants, the band was higher, with 910 bp (647 bp + 263 bp). We additionally applied exogenous GA and notice that it did not interfere with the digestion pattern in both WT and *dap*at plants (Figure 4).

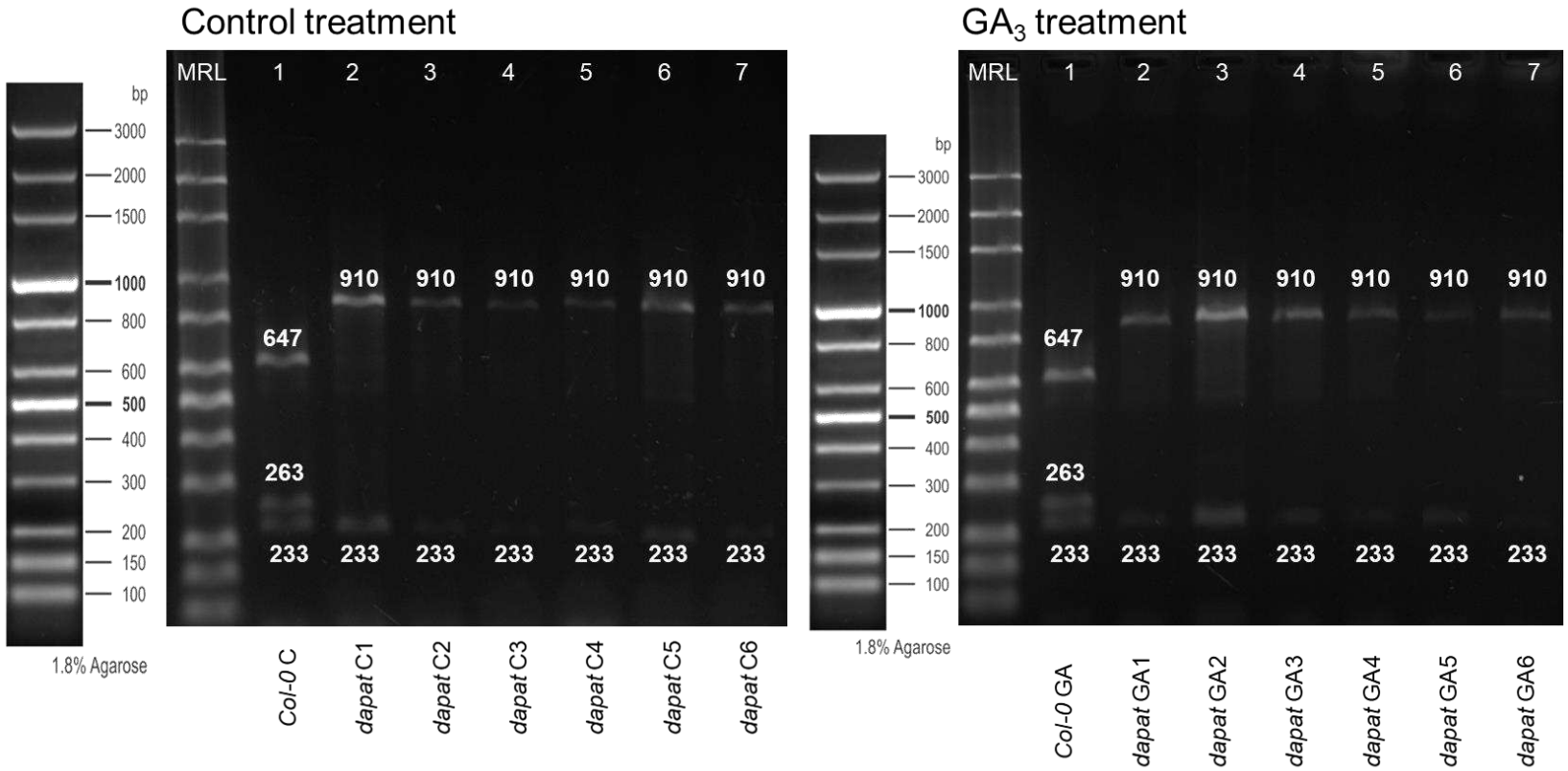

Figure 4 - *dapat* genotype was also confirmed in the shoot of control and GA-treated plants.

Genotyping of wild-type (WT, Col-0) and *dapat* plants by PCR-RFLP in 1,5% agarose TAE 1X gel. The first column was loaded with 3 µL of MRL in both gels, samples represent control and GA treated WT *Hha*I digested amplicons, and samples 2 to 7 represent control and GA_3 treated *dapat Hha*I digested amplicons. For all samples, 10 µL of digested amplicon were loaded in the wells.

4.2. Changes in plant growth under GA regime

To further investigate the impact of the DAPAT mutation on plant growth we next compared the development of WT and *dapat* plants. In consonance with previous results (CAVALCANTI et al., 2018; SONG *et al.*, 2004), *dapat* plants exhibited a reduced rosette diameter (~42% - Figure 5; Figure 6C). This was coupled with a lower total number of leaves (~73% - Figure 6D), a clear decrease in both fresh and dry weight accumulation (48% and 57% respectively - Figure 6A, B); as well, a reduction in total leaf area (~ 50%) compared to the WT plants (Figure 6E). On the other hand, we observed that exogenous GA seemingly mitigates growth impairments in the lysine deficient mutant plants. Thus, the application of GA_3 alone led to an increase in the growth of the *dapat* mutant rosette that was close to the growth of WT without GA (Figure 5). The exogenous application promotes an increase in the fresh weight accumulation (Figure 6A), rosette growth (Figure 6C), number of leaves (Figure 6D), total leaf area (Figure 6E), and specific leaf area (Figure 6F) on *dapat* plants, yet in dry weight it was not significantly (Figure 6B). Although GA_3 treatment has a positive effect on almost all parameters analyses, it had a negligible impact on the WT (Figure 5; Figure 6A-F).

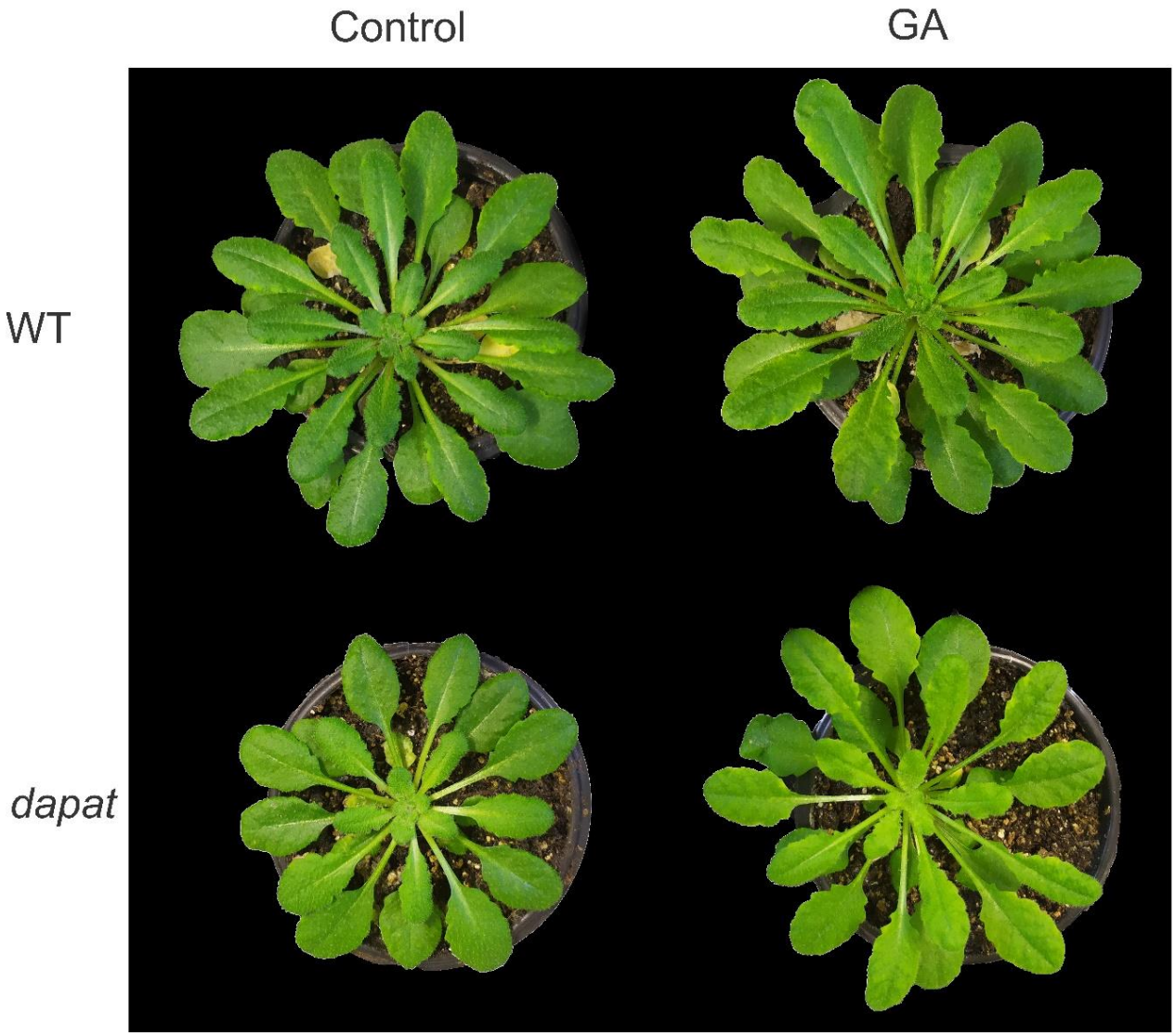

Figure 5 - GA_3 treatment partially rescues the dwarf phenotype of *dapat* mutant plants.

Representative images of 36-day-old *Arabidopsis* plants grown under short-day conditions and after further treatment with GA_3 for 14d. Further details are described in *Materials and Methods*.

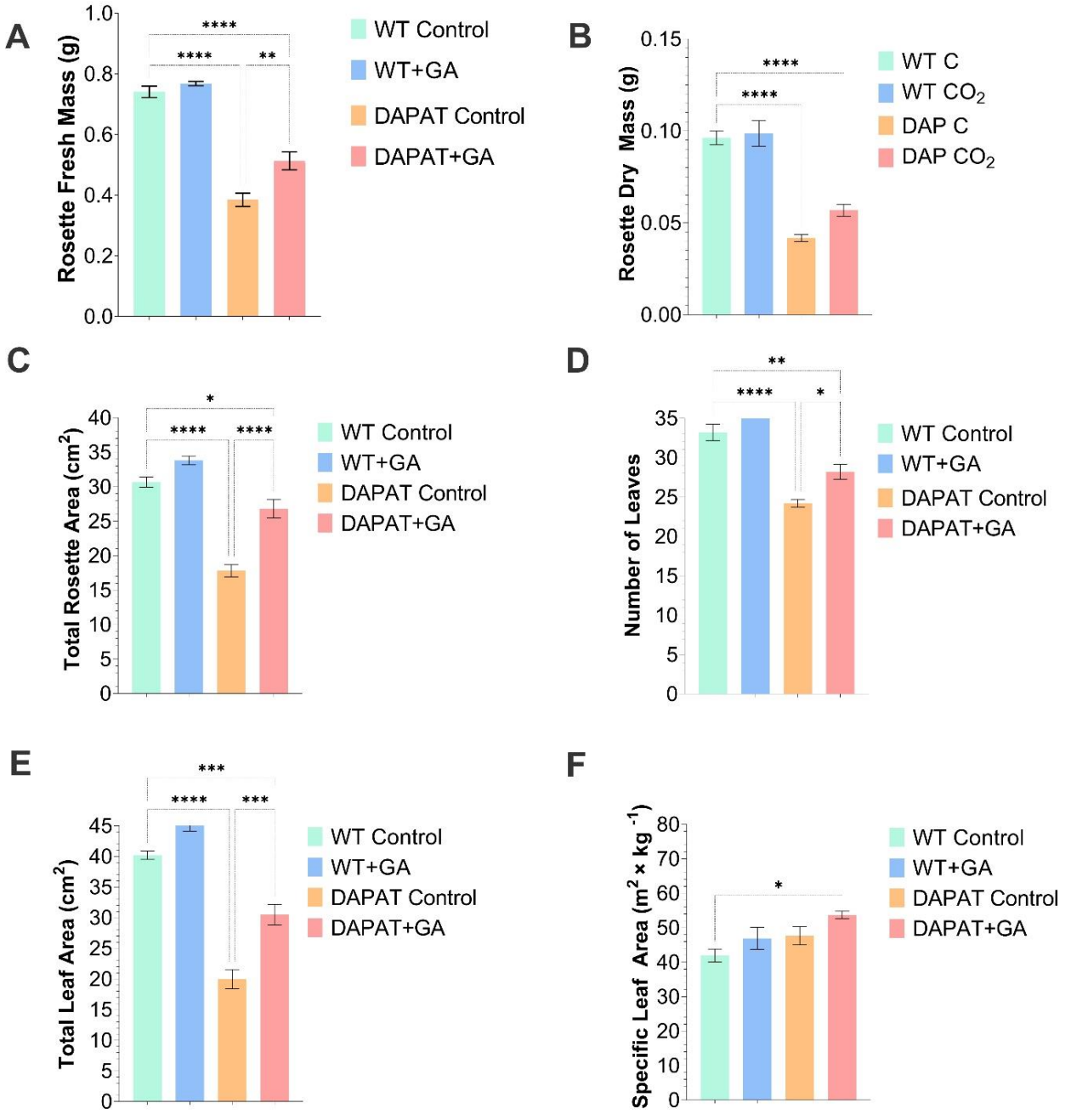

Figure 6 - GA regime positively impacts the impaired growth exhibited by the *dapat* mutant.

Biometric parameters measurements in wild-type (WT) and mutant (*dapat*) under either control conditions (Control) or following exogenous GA application (+GA). Rosette fresh mass (A), Rosette dry mass (B), Total rosette area (C), Number of leaves (D), Total leaf area, and (E) Specific leaf area. Asterisks indicate values to be significantly different by Tukey test at the 5% level, with comparisons

made in each column. The ns letters indicate values that are not statistically different. Values represent the mean ± standard error of five independent samples.

4.3. Measurements of gas exchange parameters

Due to the impact observed on the growth of *dapat* mutant plants both here (Figure 5; Figure 6) and in previous works (CAVALCANTI et al., 2018; RATE; GREENBERG, 2001; SONG, 2004), we postulate that the balance between photosynthetic and respiratory rates most likely impacted growth in response to application of GA in *dapat* mutant plant. Therefore, gas exchange measurements were performed and we observed that gas exchange parameters including net CO_2 assimilation rates (A), stomatal conductance (g_s), internal CO_2 concentration (C_i), and dark respiration (R_d) were not altered in response to either lysine biosynthesis deficiency (*dapat* mutant) or GA application (Figure 7). Accordingly, none of the evaluated parameters were affected by the application of GA in the *dapat* mutant. This fact aside, there was a significant increase in the R_d in WT plants submitted to exogenous GA application (Figure 7D).

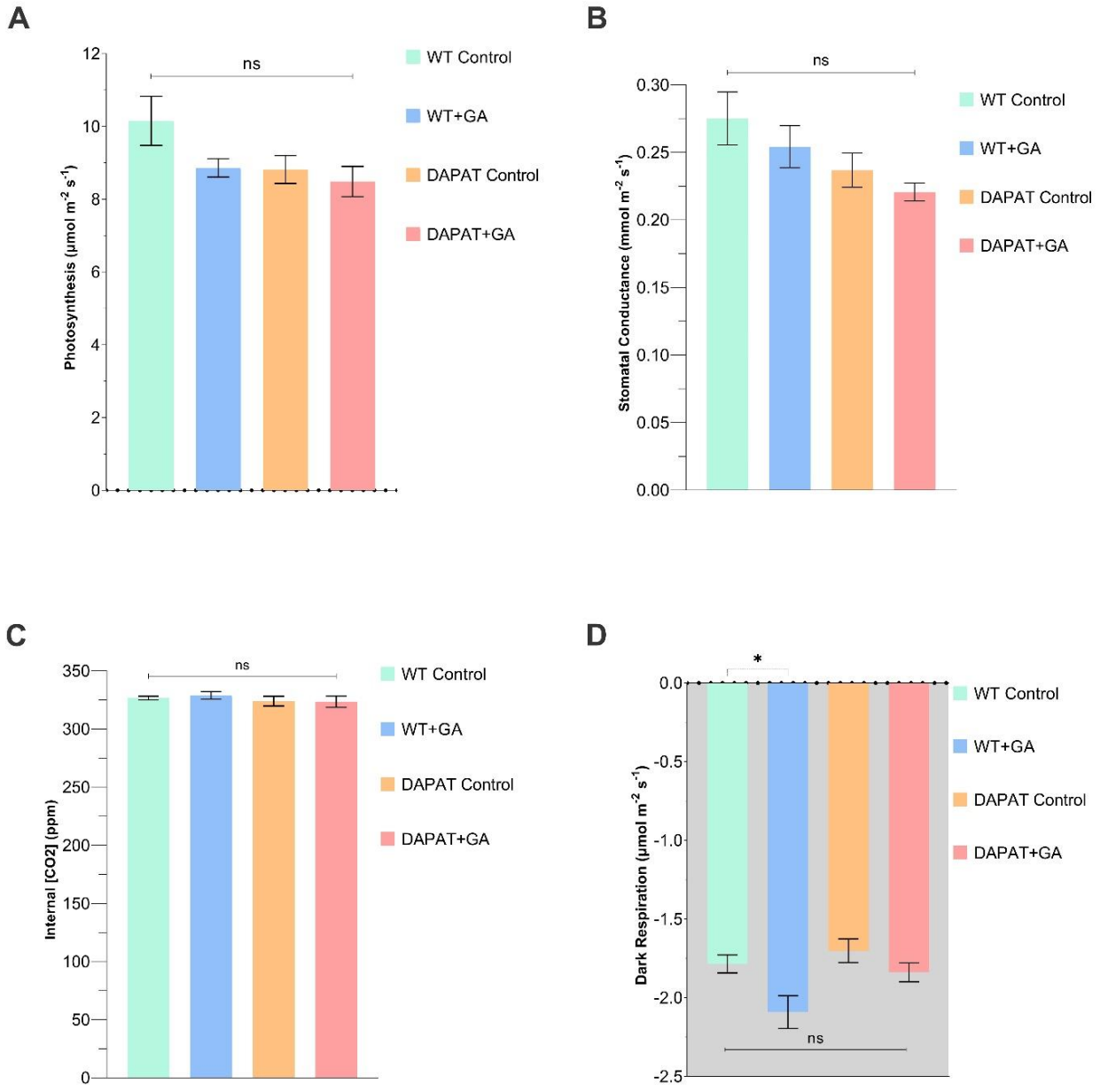

Figure 7 - Gas exchange parameters are neither affected by DAPAT mutation nor by exogenous GA treatment.

Gas-exchange measurements in wild-type (WT) and mutant (*dapat*) under either control conditions (Control) or following exogenous GA application (+GA). Photosynthesis (A), Stomatal conductance to water vapor (B), Internal CO_2 concentration (C), and Dark respiration (D). Asterisks indicate values to be significantly different by Tukey test at the 5% level, with comparisons made in each column. The ns letters indicate values that are not statistically different. Values represent the mean ± standard error of six independent samples.

4.4. Metabolic changes in response to GA application

To further understand the effect of exogenous GA on primary metabolism in *dapat* plants, the pigments, total protein, amino acids, reducing sugars, sucrose, starch, and organic acids levels were measured at the end of the day (ED) and the end of the night (EN) to assess the overall metabolic condition of the plants. Overall, the concentration of chlorophylls (*a* and *b*) decreased in WT plants under GA_3 treatment as compared with their respective control at the ED, while in *dapat* treated plants, only Chl *a* content was significantly reduced compared to the *dapat* mutant plants under control conditions. No significant difference was observed for carotenoid content and Chla/Chlb in both WT and *dapat* mutant plants (Figure 8A). A possible explanation for the reduction in the chlorophylls levels is that the leaf elongation promoted by GA_3 treatment led to a lower concentration of pigments per unit of mass in treated plants. At the EN, no difference in chlorophyll, carotenoid, and Chla/Chlb content was observed (Figure 8B).

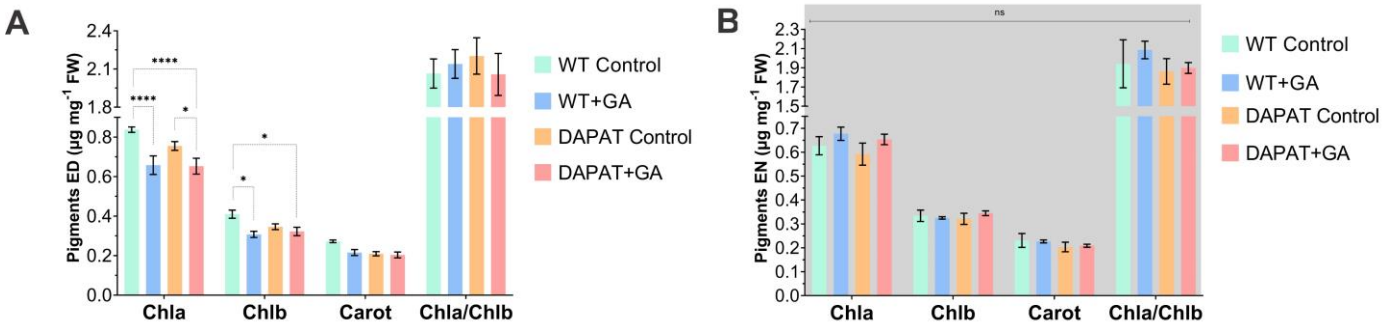

Figure 8 - GA treatment negatively impacts pigment content in both wild-type (WT) and *dapat* plants.

Variation in chlorophylls and carotenoid contents in leaves of *Arabidopsis thaliana* under either control conditions (Control) or following exogenous GA-treatment (+GA). Chlorophyll *a*, chlorophyll *b*, carotenoids, and Chla/Chlb were measured at the end of the day (A) and the end of the night (B). Asterisks indicate values to be significantly different by Tukey test at the 5% level, with comparisons made in each column. The ns letters indicate values that are not statistically different. Values represent the mean ± standard error of five independent samples.

Glucose and fructose showed a similar pattern, with lower levels in *dapat* plants in the ED and the EN (Figures 9A and 9B). Sucrose levels in *dapat* mutant plants are lower than WT plants under control conditions at the ED, however, was invariant between the mutant and WT plants at the EN (Figure 9C).

Our results revealed a higher starch breakdown in *dapat* mutant (Figure 9D), demonstrated by the equal levels of starch compared to the WT control at the ED, with a low starch content at nighttime (EN). These results indicate that the impact in the lysine biosynthesis pathway most likely promoted sugar starvation at night (CAVALCANTI et al., 2018).

Glucose, fructose, sucrose, and starch levels in WT plants under control conditions were similar to those under exogenous GA at both sampling times (Figure 9A-D).

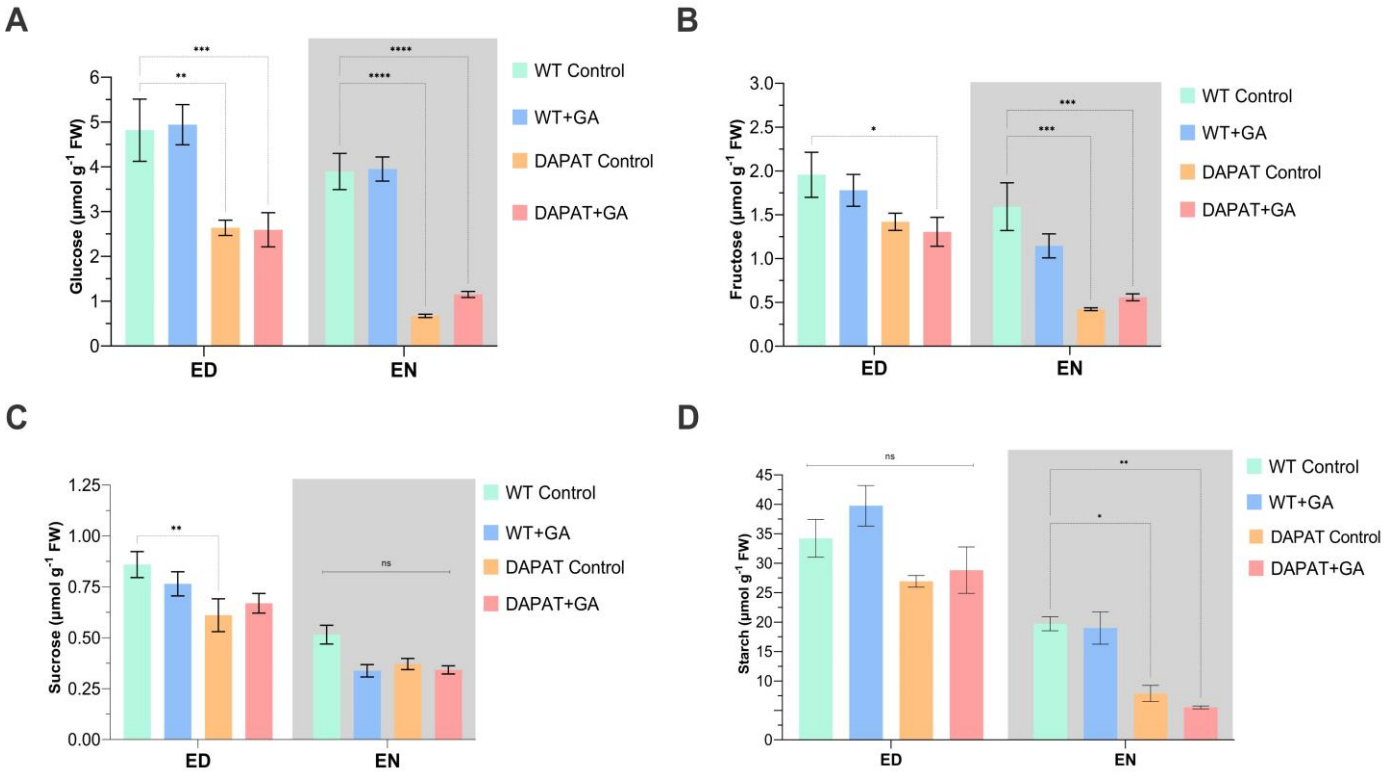

Figure 9 - The carbohydrate levels are drastically reduced in the nighttime in *dapat* plants.

Variation in the carbohydrate content in *Arabidopsis thaliana* under either control conditions (Control) or following exogenous GA-treatment (+GA). Glucose (A), Fructose (B), Sucrose (C), and Starch (D) were measured at the end of the

day (white background) and the end of the night (gray background). Asterisks indicate values to be significantly different by Tukey test at the 5% level, with comparisons made in each column. The ns letters indicate values that are not statistically different. Values represent the mean ± standard error of five independent samples.

The analysis of the levels of nitrogenous compounds revealed a virtually invariable content of protein in WT and *dapat* plants regardless of growth conditions at both ED and EN (Figure 10A). By contrast, high amino acid levels were observed in *dapat* plants compared to the WT under control conditions, at the ED (Figure 10B). Although exogenous GA treatment did not affect total protein content in *dapat* treated plants, it is noteworthy that there was increased amino acids content at night in mutant plants compared to its respective control (Figure 10B).

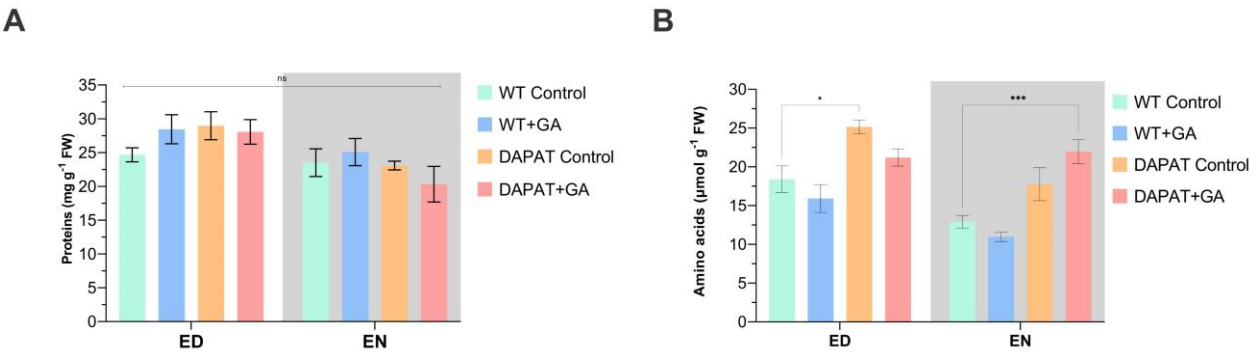

Figure 10 - DAPAT mutation triggers a high amino acid turnover in mutant plants.

Variation in the nitrogen compounds content in *Arabidopsis thaliana* under either control conditions (Control) or following exogenous GA-treatment (+GA). Protein (A), and Amino acids (B) were measured at the end of the day (white background) and the end of the night (gray background). Asterisks indicate values to be significantly different by Tukey test at the 5% level, with comparisons made in each column. The ns letters indicate values that are not statistically different. Values represent the mean ± standard error of five independent samples.

Decrease levels of malate were observed in *dapat* mutant plants at the ED compared with WT plants, whilst similar levels between genotypes and growth conditions were observed at the EN (Figure 11A). Remarkably, significantly decreased levels of fumarate

were observed in *dapat* mutant plants at both ED and EN (Figure 11B). Our results also showed that the levels of organic acids were not affected by exogenous GA-treatment in both genotypes (Figure 11A, B).

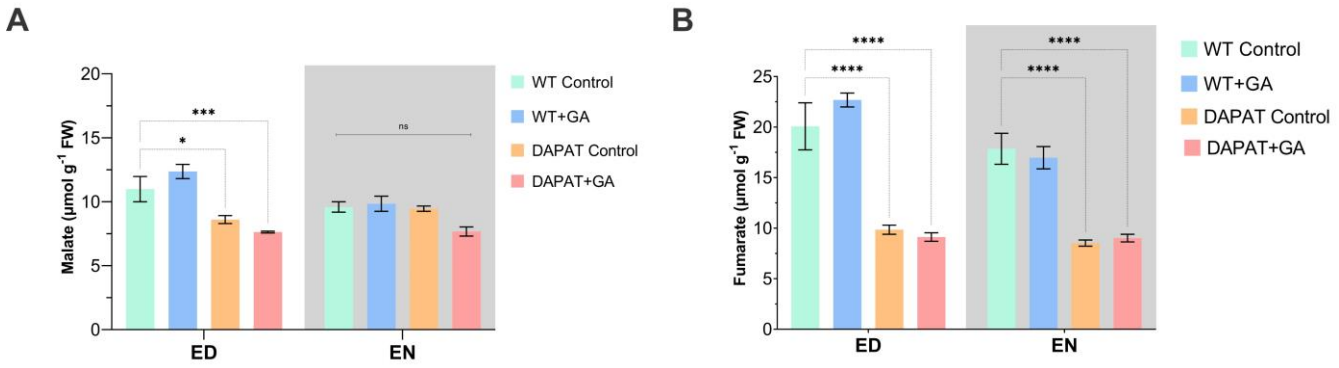

Figure 11 - DAPAT mutation promotes a reduction in organic acid levels.

Variation in the content of the organic acids in *Arabidopsis thaliana* under either control conditions (Control) or following exogenous GA-treatment (+GA). Malate (A) and Fumarate (B) were measured at the end of the day (white background) and the end of the night (gray background). Asterisks indicate values to be significantly different by Tukey test at the 5% level, with comparisons made in each column. The ns letters indicate values that are not statistically different. Values represent the mean ± standard error of five independent samples.

4.5. Gene expression

The ability of GA_3 to partially rescue the dwarf phenotype of *dapat* mutant plants suggested that the synthesis of such hormone may be impacted. To investigate the contribution of GA biosynthesis in the phenotype of the deficient lysine biosynthesis *dapat* mutant, five representative genes of GA biosynthesis were selected and their relative expression was examined by RT-qPCR. The Log_2 Fold Change (FC) was calculated based on the relative expression values (normalized by the values found for WT control plants) shown in Figures 12 and 13.

It was observed a 2-fold reduction in the transcript levels of *KS* in *dapat* control when compared to WT at the ED (Figure 12). Similarly, the majority of the analyzed GA-related genes (e.g. *KS*, *KO,* and *GA20ox1*) were 2 to 4 fold less abundant in GA-treated

plants. This fact aside, genes associated with the beginning (*CPS*) and the end (*GA3ox1*) of the GA biosynthesis pathway were characterized by increased levels such as an increased level of *GA3ox1* in the *dapat* mutant plants under control conditions. Since *CPS* acts at the beginning of the GA biosynthesis pathway, the fine control of its expression may act as a trigger in this pathway.

In light of the aforementioned impact in the levels of carbohydrate and nitrogen compounds, analyses of the relative transcript levels of *LKR/SDH*, *IVDH*, *D2HGDH,* and *ETFQO* were also performed. At the ED, *LKR/SDH* and *IVDH* were at least 2-fold less abundant in all plants in comparison to WT plants under control conditions, showing the effect of GA application (Figure 12). It is important to mention that *D2HGDH* and *ETFQO* expression levels did not differ from the WT regardless of the genotype and growth condition (Figure 12).

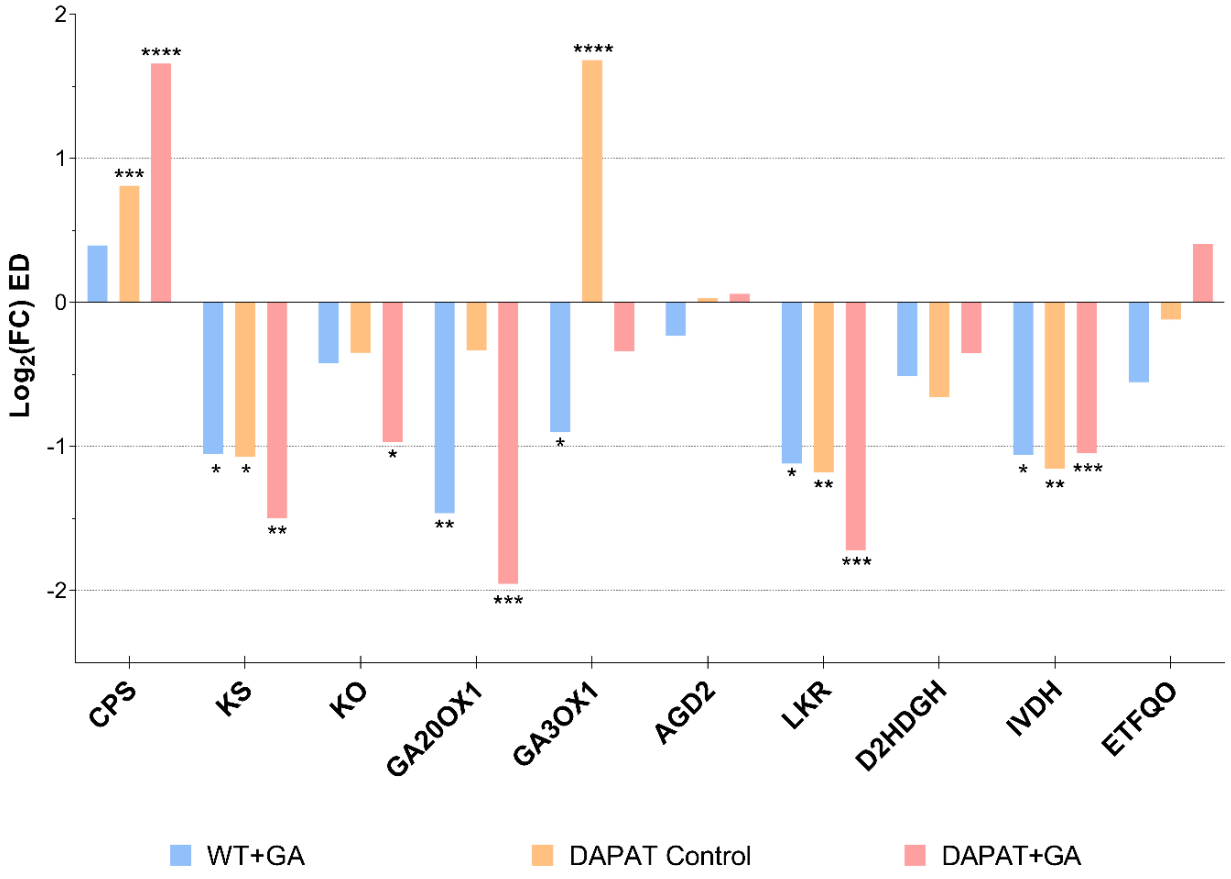

Figure 12 - DAPAT mutation causes the significant differential-expression of *CPS*, *KS*, and *GA3ox1* genes of GA biosynthesis at the ED.

Changes in the expression levels of genes encoding enzymes involved GA biosynthesis and amino acids metabolism in *Arabidopsis thaliana* under either control conditions (Control) or following exogenous GA-treatment (+GA). RT-qPCR analysis of transcript levels of *CPS* gene (At4g02780), *KS* (At1g79460), *KO* (At5g25900), *GA20ox1* (At4g25420), *GA3ox1* (At1g15550), *AGD2 (*At4g33680), *LKR/SDH (*At4g33150), *D2HGDH (*At4g36400), *IVDH (*At3g45300), *ETFQO (*At2g43400). Expression levels are expressed as Log_2 Fold Change at the end of the day (A). Data are mean of three replicates (± SEM). Asterisks indicate significant differences compared to the wild-type control at < 5% (*), < 1% (**), < 0.1% (***) and < 0.01% (****) confidence levels, respectively. Further details are additionally available in Supplemental Figure 1 for RT-qPCR analysis of relative transcript levels of genes described above.

The same genes comprising GA biosynthesis, lysine biosynthesis/degradation, and alternative respiratory pathways were also evaluated at the EN (Figure 13). In *dapat* mutant plants, the levels of *CPS, KS*, *KO*, and *GA20ox1* did not differ from their WT counterpart, with a slight down-regulation on *KO* and *GA20ox1* in *dapat* plants treated with GA_3. However, upon GA_3 treatment, *GA3ox1* was highly down-regulated in both WT (~5.4-fold) and *dapat* (~3.5-fold) plants. By contrast, at the EN, it was observed that LKR/*SDH* expression was ~1.9-fold up-regulated in WT GA_3 treated plants, whereas the expression of *D2HDGH*, *IVDH,* and *ETFQO* showed a subtle tendency to be down-regulated in both controls and GA_3 treated plants (Figure 13).

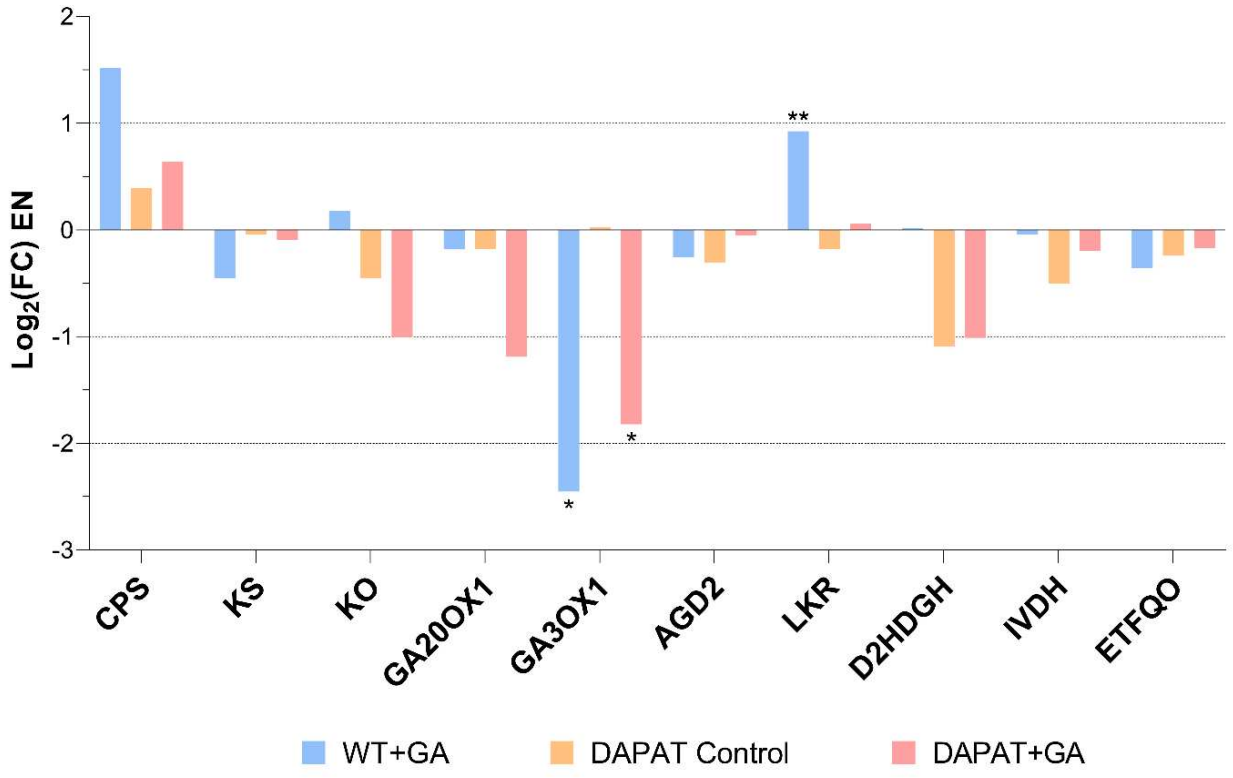

Figure 13 - The expression of *GA3ox1* is modified at the EN for *dapat* mutant plants, which is further enhanced upon GA_3 treatment.

Changes in the expression levels of genes encoding enzymes involved GA biosynthesis and amino acids metabolism in *Arabidopsis thaliana* under either control conditions (Control) or following exogenous GA-treatment (+GA). RT-qPCR analysis of transcript levels of *CPS* gene (At4g02780), *KS* (At1g79460), *KO* (At5g25900), *GA20ox1* (At4g25420), *GA3ox1* (At1g15550), *AGD2 (*At4g33680),

*LKR/SDH (*At4g33150)*, D2HGDH (*At4g36400)*, IVDH (*At3g45300)*, ETFQO (*At2g43400). Expression levels are expressed as Log_2 Fold Change at the end of the night (EN). Data are mean of three replicates (± SEM). Asterisks indicate significant differences compared to the wild-type control at < 5% (*), < 1% (**), < 0.1% (***) and < 0.01% (****) confidence levels, respectively. (Further details are additionally available in Supplemental Figure 1 for RT-qPCR analysis of relative transcript levels of genes described above).

Given the impaired growth observed in *dapat* mutant plants coupled with the marked reduction in carbohydrate levels in *dapat* mutant plants either under control or following GA treatment, we measured the expression levels of *DIN6* (FUJIKI et al., 2001) and *ATL8* (GRAF et al., 2010; LUO et al., 2019) as starvation-related genes. Briefly, we were able to assess the extent of the starvation symptoms triggered by the DAPAT mutation. First, we observed that the expression of the *DIN6* gene was virtually invariant between genotypes and growth conditions at the ED (Figure 14A). By sharp contrast, the expression level of *DIN6* at the EN was strongly elevated in *dapat* mutant plants, indicating that sugar starvation was indeed occurring in the leaves of the mutant even under optimal control conditions. Interestingly, *DIN6* expression was even higher following GA_3 treatment in *dapat* plants, indicating that exogenous GA promoted enhanced starvation in the mutant, most likely as a result of the observed growth increment under this condition. In contrast, such an effect was not observed in WT plants following GA treatment, since the expression for *DIN6* was not altered (Figure 14A).

Sugar starvation for mutant plants at night was reinforced by the expression levels of *ATL8.* We observed that the expression of the *ATL8* gene, like the *DIN6* gene (Figure 14A), was invariant between genotypes and growth conditions at the ED (Figure 14B). However, the expression level of *ATL8* at the EN was significantly elevated in *dapat* mutant plants, especially for control plants in this case (Figure 14B). Thus, indicating that sugar starvation was indeed occurring in leaves of mutant plants, triggered by the DAPAT mutation.

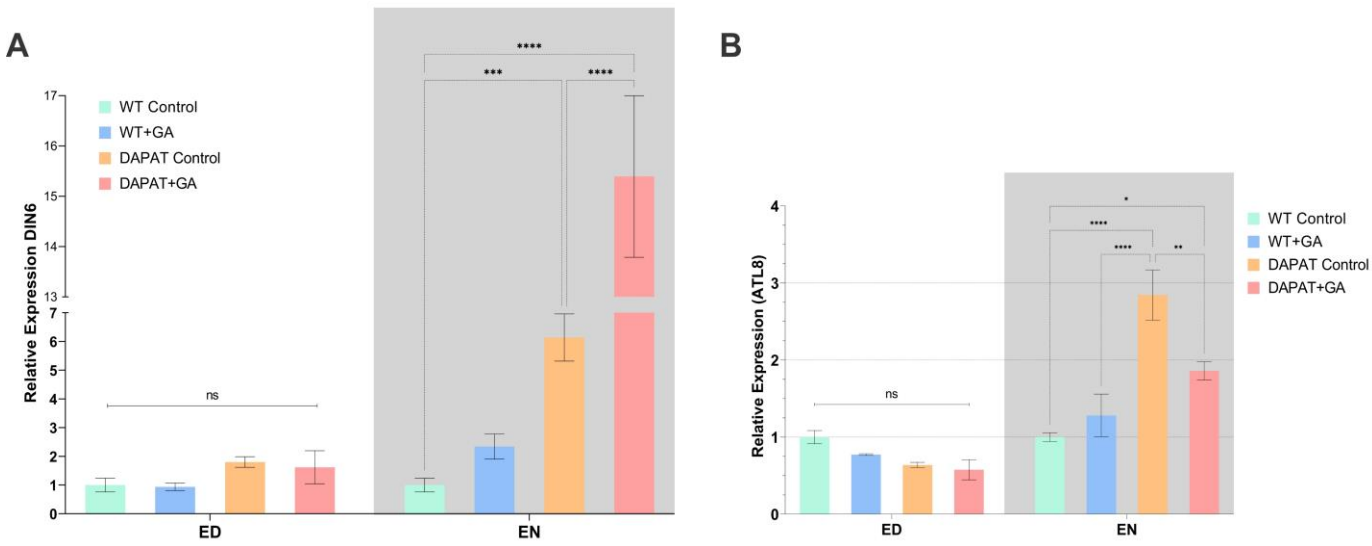

Figure 14 - *DIN6* and *ATL8* are enriched in the *dapat* mutant at the EN.

Relative expression of *DIN6* and *ATL8* as markers of the sugar starvation process. Comparisons of the expression of the starvation reporter genes *DIN6* (A) and *ATL8* (B) in *Arabidopsis thaliana* under either control conditions (Control) or following exogenous GA-treatment (+GA). The relative expression level (REL) at the end of the day (ED) and night (EN) of the WT was set to 1. Data are mean of three replicates (± SEM). Asterisks indicate significant differences compared to the wild-type control at < 5% (*), < 1% (**), < 0.1% (***) and < 0.01% (****) confidence levels, respectively.

4.6. Protein-protein interaction network analyses

Protein-protein interaction networks were performed with the online tool STRING version 11.5 (https://string-db.org/) (SZKLARCZYK et al., 2021). Through this approach, we seek to investigate co-expression and co-occurrence partners of the *A. thaliana glutamine-dependent asparagine synthase 1* (*ASN1*) - a.k.a *DIN6*, and *AT1G76410* - a.k.a *ATL8* in an attempt to establish the regulation pattern of these genes in *dapat* mutant plants.

In this protein-protein network, the OGC parameter indicates how many proteins are annotated with a particular biological process within the network. Low FDR values indicate that these biological processes are significantly connected with the candidate

gene (*DIN6* and *ATL8*). The network strength indicates the Log10 of the ratio between the number of proteins annotated to each biological process and the number of expected proteins to be annotated with the same biological process in a random network of the same size. The higher this value is, the greater is the number of significant interactions associated with the biological process.

DIN6 was up-regulated in *dapat* mutant plants regardless of growth conditions (control and upon GA treatment) (Figure 14A), to summarize, the *DIN6* network allowed us to evidence the role of *ASN1* (*DIN6*) as noticed by its co-expression with several queried genes, including *ASS, AK-LYS1, AK2, AK3, PYRB, ADSS, STR15, ASP5,* and *ASP2*. As would perhaps be expected, this co-expression analysis revealed close connections between the candidate and the query genes. Interestingly, the majority of those genes, whose function has been experimentally investigated, showed strong transcriptional regulation with the candidate gene, *DIN6* (Figure 15). These proteins are involved in the metabolism of amino acids, *de novo* pyrimidine biosynthesis, nitrogen mobilization, and senescence in land plants.

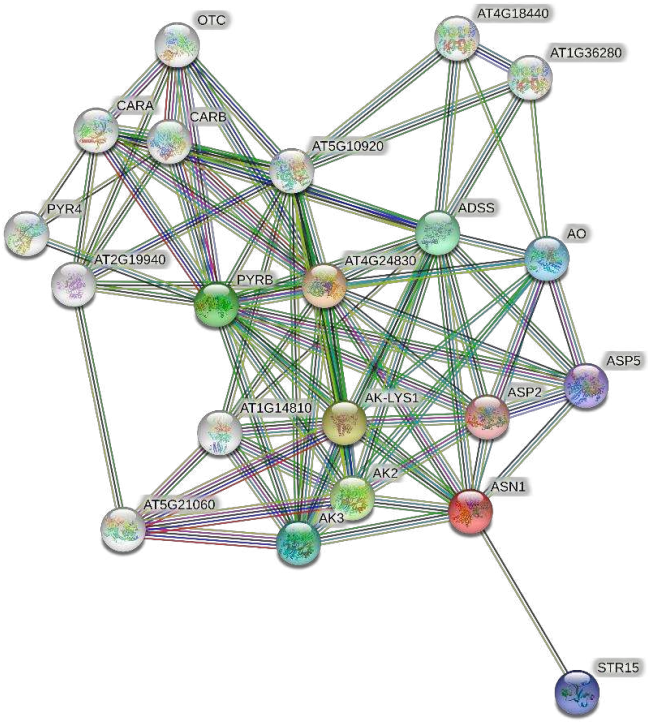

GO-term	Description	Count in network	Strength	FDR
GO:0000050	Urea cycle	4 of 6	2.94	5.66e-10
GO:0044205	'De novo' UMP biosynthetic process	4 of 6	2.94	5.66e-10
GO:0042450	Arginine biosynthetic process via ornithine	2 of 3	2.94	1.32e-05
GO:0006526	Arginine biosynthetic process	6 of 12	2.81	4.64e-14
GO:0006103	2-oxoglutarate metabolic process	2 of 5	2.72	2.64e-05
GO:0009088	Threonine biosynthetic process	3 of 8	2.69	2.65e-07
GO:0006207	'De novo' pyrimidine nucleobase biosynthetic process	3 of 9	2.64	3.46e-07
GO:0006531	Aspartate metabolic process	2 of 7	2.57	4.23e-05
GO:0009089	Lysine biosynthetic process via diaminopimelate	3 of 14	2.45	8.49e-07
GO:0046132	Pyrimidine ribonucleoside biosynthetic process	4 of 20	2.42	1.65e-08
GO:0009064	Glutamine family amino acid metabolic process	9 of 64	2.26	7.35e-17
GO:0009066	Aspartate family amino acid metabolic process	6 of 59	2.12	8.32e-11

Figure 15 – *DIN6* is related to carbon-starvation perception and amino acids catabolism.

STRING protein-protein interaction network of *DIN6* (*ASN1*) with its top 12 strongest GO terms for biological process**.** Each node represents proteins produced

by a single, protein-coding gene locus (spliced isoforms and PTMs are collapsed). Node color: Colored nodes are query proteins and the first shell of interactions; white nodes are proteins of the second shell of interactions. Node content: empty nodes are proteins of unknown 3D structures and filled nodes represent some of the known/predicted 3D structures. Edges represent protein-protein associations meant to be specific and meaningful, this does not necessarily mean they are physically binding each other. Known interactions are shown as cyan (from curated databases) or pink edges (experimentally determined). There are 3 types of predicted interactions; gene neighborhood (green edge), gene fusions (red edge), and gene co-occurrence (dark-blue edge). Other types of interactions are those assigned for text mining (light green edge), co-expression (black edge), and protein-homology (light blue edge). FDR (false discovery rate), modification (post-translational modifications).

ATL8 that encodes a member of the *Arabidopsis* Tóxicos en Levadura (ATL) family (LUO et al., 2019) was significantly up-regulated in *dapat* mutant plants regardless of growth conditions (control and upon GA treatment) (Figure 14B). Briefly, the *ATL8* network allowed us to evidence the role of *ATL8 (AT1G76410)* as noticed by its co-expression with several queried genes, including *AT5G63620, ETFQO, ALDH6B2, THA1, PP2-A13, AKINBETA1 (*SnRK1 subunit*), AT1G18270,* and *PSK2*. As would perhaps be expected, this co-expression analysis revealed close connections between the candidate and the query genes. Interestingly, the majority of those genes, whose function has been experimentally investigated, showed strong transcriptional regulation with the candidate gene, *ATL8* (Figure 16). These proteins are involved in the glyceraldehyde-3-phosphate biosynthesis, glycerol catabolism, leucine catabolism, gluconeogenesis, photoperiodism, nonsense mediated decay of mRNA and mRNA transport.

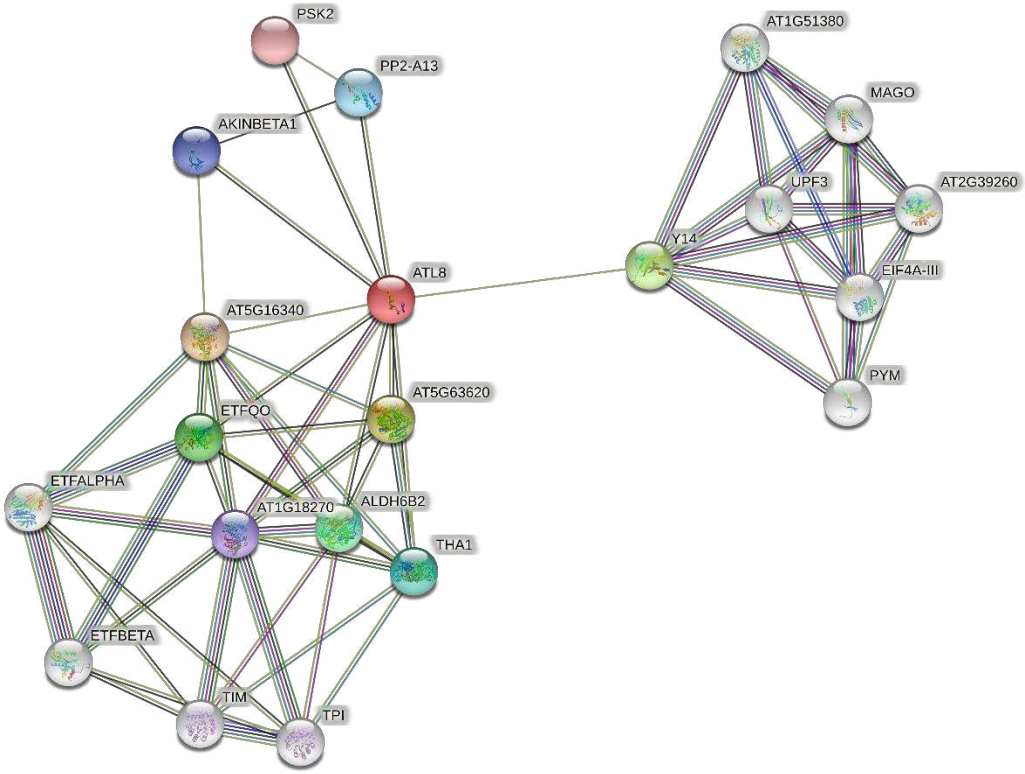

GO-term	Description	Count in network	Strength	FDR
GO:0046166	Glyceraldehyde-3-phosphate biosynthetic process	2 of 2	3.12	0.0016
GO:0019563	Glycerol catabolic process	2 of 4	2.81	0.0038
GO:0006552	Leucine catabolic process	2 of 6	2.64	0.0061
GO:0000184	Nuclear-transcribed mRNA catabolic process, nonsense-mediated decay	6 of 21	2.57	4.66e-10
GO:0048571	Long-day photoperiodism	2 of 17	2.19	0.0304
GO:0006094	Gluconeogenesis	2 of 18	2.16	0.0331
GO:0051028	mRNA transport	5 of 70	1.97	3.50e-06
GO:0034655	Nucleobase-containing compound catabolic process	8 of 168	1.79	1.34e-09
GO:1901606	Alpha-amino acid catabolic process	3 of 64	1.79	0.0066
GO:0046700	Heterocycle catabolic process	9 of 214	1.74	4.66e-10
GO:0044270	Cellular nitrogen compound catabolic process	9 of 214	1.74	4.66e-10
GO:0019439	Aromatic compound catabolic process	9 of 238	1.69	4.66e-10

Figure 16 – *ATL8* is co-expressed with sugar-starvation signaling proteins.

STRING protein-protein interaction network of *ATL8* (*AT1G76410*) with its strongest GO terms for biological process. Each node represents proteins produced by a single, protein-coding gene locus (spliced isoforms and PTMs are collapsed). Node color: Colored nodes are query proteins and the first shell of interactions; white nodes are proteins of the second shell of interactions. Node content: empty nodes are

proteins of unknown 3D structures and filled nodes represent some of the known/predicted 3D structures. Edges represent protein-protein associations meant to be specific and meaningful, this does not necessarily mean they are physically binding each other. Known interactions are shown as cyan (from curated databases) or pink edges (experimentally determined). There are 3 types of predicted interactions; gene neighborhood (green edge), gene fusions (red edge), and gene co-occurrence (dark-blue edge). Other types of interactions are those assigned for text mining (light green edge), co-expression (black edge), and protein-homology (light blue edge). FDR (false discovery rate), modification (post-translational modifications).

5. DISCUSSION

Lysine is an essential amino acid and its metabolism is closely associated with the TCA cycle and the mETC (ARAUJO et al., 2010; GALILI, 2011). Moreover, it is also involved in plant stress responses in several distinct ways (YANG; ZHAO; LIU, 2020). The significance of lysine in plant metabolism can be inferred from the fact that loss of the DAPAT gene, which encodes for one of the lysine biosynthesis enzymes, the *L,L*-diaminopimelate aminotransferase (*L,L*-DAPAT) in *A. thaliana* homozygous knockout mutants is lethal at the embryo level (SONG, 2004), suggesting the gene essentiality. Furthermore, a single amino acid substitution in the *L,L*-DAPAT gene in *A. thaliana* resulted in a marked reduction in enzyme activity that led to a lower resistance against *Pseudomonas syringae*, as well as dwarfism, accumulation of salicylic acid, and alteration of leaf morphology in *dapat* mutant plants (RATE; GREENBERG, 2001; SONG, 2004). We first demonstrate that the chemical point mutation in the DAPAT gene, which encodes for the *L,L*-DAPAT enzyme, promotes a missense in the translated protein (Figure 3 and Figure 4), without affecting the expression of the gene itself either at ED or EN (Figure 12 and Figure 13).

It has been previously demonstrated that the metabolic, protein and transcriptional profiles of *dapat* plants under optimal growth conditions are directly related to patterns observed in plants under stress conditions (CAVALCANTI et al., 2018). Thus, the growth inhibition triggered by the DAPAT mutation is associated with an extensive metabolic reprogramming that simulates a putative stress condition in the mutant plants

(CAVALCANTI et al., 2018). Although the specific molecular mechanism that triggers such an energy-limiting scenario has not been fully characterized, here we first observed that the impaired growth phenotype observed in the *dapat* mutant is seemingly mitigated by exogenous GA application. Thus, the present work investigated the physiological and metabolic responses of an *A. thaliana* mutant for the lysine biosynthesis enzyme *L,L*-DAPAT following exogenous GA treatment.

The dramatic reduction of *L,L*-DAPAT enzyme activity affected the shoot development in *A. thaliana* (Figure 5)(CAVALCANTI et al., 2018; SONG, 2004). Our results are in good agreement with those previously obtained from the characterization of the *dapat* mutant under control conditions, which also exhibited delayed germination kinetics (CAVALCANTI et al., 2018), as well as delayed flowering. Similar traits have also been observed in mutants defective in GA synthesis or signaling in different plant species (HEDDEN; THOMAS, 2012; RIBEIRO et al., 2012).

Following GA treatment, *dapat* plants responded positively with a partial rescue of the dwarf phenotype observed under optimal growth conditions (Figure 5). This fact aside, there was no significant increase in RDM (Figure 6B), indicating that the GA_3 application promoted leaf elongation and shoot growth without the rescue of impaired carbon metabolism (PAPARELLI et al., 2013), previously observed in *dapat* mutant plants (CAVALCANTI et al., 2018).

The absence of significant effects on A, g_s, and R_d under either control conditions or following GA_3 application (Figure 7), provides further evidence that the biomass reduction cannot be directly connected with gas exchange limitations (PAPARELLI et al., 2013; RIBEIRO et al., 2012).

Previous metabolic analyses highlighted a scenario of energy limitation triggered by the DAPAT mutation (CAVALCANTI et al., 2018). Although GA_3 treated *dapat* mutant plants exhibited similar levels of carbohydrates compared to their respective control at the time points evaluated, there was a trend toward increased content of reducing sugars (Figure 9A, B) at night, as opposed to a lower starch level (Figure 9D) for the same time point. Thus, there is an indication of a possible detour of photosynthates to fuel growth triggered by GA in *dapat* mutant plants, and to the detriment of starch synthesis

(PAPARELLI et al., 2013), an effect that was not observed in WT plants following GA_3 application.

During carbon starvation, general catabolic events are activated, and the protein catabolism with the subsequent oxidation of amino acids produces the energy either required to fuel particular needs of certain organs or used as alternative substrates to sustain mitochondrial respiration and ATP synthesis (ARAÚJO et al., 2011; HILDEBRANDT et al., 2015). Notably, the observed increase in free amino acid content in *dapat* mutant plants is closely associated with the sugar deficits exhibited by *dapat* plants especially at night. The increase of free amino acids provides further evidence of the occurrence of a clear C/N imbalance due to the dramatic reduction in *L,L*-DAPAT activity, which does not seem to be attenuated by the application of exogenous GA.

Fumarate can accumulate to high levels in leaves of *Arabidopsis* (CHIA et al., 2000). It has been also recognized as an important respiratory substrate, especially in situations of low carbohydrate concentration (ARAÚJO et al., 2011; GIBON et al., 2009), and it has been described as a carbon source in several species for growth maintenance (ARAÚJO et al., 2012). Such reduced levels of fumarate in *dapat* plants (Figure 11B) probably indicate a preferential usage of amino acids as alternative substrates, as depicted by the maintenance of their high levels in mutant plants (Figure 10B), with fumarate being most likely directed to the maintenance of amino acid synthesis. It seems reasonable to assume that this metabolic response could be another metabolic adjustment used by *dapat* plants to sustain growth facing such carbon starvation stress linking fumarate and amino acid metabolism (PRACHAROENWATTANA et al., 2010).

Lysine is an important substrate for alternative respiration by providing electrons to the ETF/ETFQO complex through its catabolism by either D2HGDH or LKR/SDH to support plant cell ATP production mainly under carbon-deficit conditions (ARAÚJO et al., 2011; GALILI et al., 2014; HILDEBRANDT et al., 2015). At the ED, the expression of genes closely related to amino acid catabolism *LKR/SDH* and *IVDH* were significantly down-regulated in all genotypes and growth conditions (Figure 12). Moreover, the expression levels of *D2HDGH* and *ETFQO* did not differ from the WT in all groups of plants at either the ED or the EN (Figures 12 and Figure 13).

We further observed that GA application was able to partially reverse the impaired growth of *dapat* plants suggesting that the *L,L*-DAPAT mutation might be associated with a differential expression for genes involved in GA synthesis, a hypothesis that was further confirmed (Figure 12 and Figure 13). The expression of *ent-kaurene synthase* (*KS*) was 2-fold reduced at the ED for *dapat* mutant plants under control conditions (Figure 12). According to Paparelli *et al.* (2013), *KS* expression is characterized by a distinct pattern of other genes involved in the GA biosynthesis pathway during the diurnal cycle. Briefly, the *KS* gene expression peaked in the afternoon, a situation that is compatible with high *ent-kaurene* levels seen in the WT at the ED (PAPARELLI et al., 2013). The reduction in the expression of *KS* in *dapat* mutant plants under control conditions can be explained, at least partially, by the altered nighttime carbohydrate metabolism, which has been shown for this mutant (Figure 9). The considerable down-regulation of *KS* is also observed following GA-treatment, being striking for *dapat* plants (Figure 12), providing further evidence that sugar starvation at night negatively affects *KS* expression during the light period (PAPARELLI et al., 2013).

Our data also demonstrated that the *copalyl diphosphate synthase* (*CPS*) was up-regulated in *dapat* plants, mainly in GA_3 treated-plants, which can be explained through the limitation caused by the low *ent-kaurene* production (FLEET et al., 2003), in agreement with the significant *KS* down-regulation in *dapat* mutant plants (Figure 12). By acting as a gateway controlling the flux of metabolites into the GA biosynthesis pathway, CPS is a key enzyme, generally low expressed due to its regulatory role (HEDDEN, 2016). Furthermore, the expression levels of *Gibberellin 20 oxidase 1* (*GA20ox1*), which is under circadian control (HISAMATSU et al., 2005), and *Gibberellin 3-beta-dioxygenase 1* (*GA3ox1*), were down-regulated in GA_3 treated plants. This fact aside, for control *dapat* plants, *GA3ox1* was expressively up-regulated (Figure 12). This result is consistent with the feedback regulation observed for three of the five *GA20ox* genes in *Arabidopsis* following GA_3 treatment (RIEU et al., 2007), and in GA-deficient dwarf mutants (MARTIN et al., 1996), whereas the up-regulation of *GA3ox1* endorse previous findings pointing to the presence of different mechanisms of feedback regulation for *GA20ox1* and *GA3ox1* in *Arabidopsis thaliana* (HEDDEN, 2016).

Finally, the expression of *DIN6*, a dark-induced and starvation-induced gene (At3g47340) (FUJIKI et al., 2001), was analyzed. Notably, it is also known as the *glutamine-dependent asparagine synthase 1* (*ASN1*) (LAM HON MING; PENG; CORUZZI, 1994). *DIN6* was differentially expressed only at night, with an expressive up-regulation in *dapat* mutant plants under control, and markedly even more up-regulated in response to GA treatment in *dapat* plants (Figure 14A). The expression levels of *DIN6* in *A. thaliana* is tightly regulated by both environmental factors and metabolites, with transcripts are strongly induced upon the initiation of sugar starvation, as in senescence leaves, to provide asparagine as nitrogen transport and/or storage compound, when carbon resources are limited (GONZALI et al., 2006; IZUMI et al., 2013; LAM; HSIEH; CORUZZI, 1998).

During senescence, nutrients such as nitrogen and others are reallocated from source leaves to sink tissues (e.g. meristem, fruit, and seeds), and therefore, proteins and amino acids are highly degraded to feed respiration as alternative substrates. In such conditions that led to amino acids depletion, the proteasome and autophagy degrade proteins to supply catabolic reactions with amino acids (ARAÚJO et al., 2011).

The role of autophagy, previously implicated in amino acids release in *Arabidopsis* during starvation conditions at night (IZUMI et al., 2013), may exert an essential physiological function in protein turnover in *dapat* mutant plants. It is important to mention that, as already evidenced by BARROS et al., (2017), that autophagy deficiency compromises protein degradation and the availability of amino acids that would be used as alternative substrates to sustain plant respiration (BARROS et al., 2017). In light of this, further studies are required to certainly confirm the connections between the lysine biosynthetic pathway and autophagy under carbon starvation or environmental stresses.

Additionally, the RING-type ubiquitin ligase *ATL8* (*AT1G76410*) had its protein-protein network (Figure 16) accessed due to its up-regulation at the EN in the *dapat* mutant (Figure 14B). *ATL8* was differentially expressed only at night, with an expressive up-regulation in *dapat* mutant plants under control (Figure 14B). This family of genes is supposed to be involved in sugar response since its expression is increased under dark conditions, and decreased by light exposure (LUO et al., 2019), or exogenous sucrose

treatment (SATO et al., 2011). As *ATL8* is a ubiquitin ligase, it could mark sugar-repressed proteins to the ubiquitin-proteasome system (UPS) in response to the carbon and putative nitrogen-starvation status of *dapat* mutant plants. Other important evidence found in the protein-protein interaction network is that sucrose non-fermenting-related kinase 1 (SnRK1) is co-expressed with *ATL8.* SnRK1 is an important component involved in sugar signalling, acting as a central regulator in response to the unbalance in the carbon homeostasis, besides, its activity is modulated by the binding with trehalose-6 phosphate which reaffirms its role in sugar-sensing in *Arabidopsis* (ZHAI et al., 2018).

Collectively, the data obtained here provide compelling evidence that the *L,L*-DAPAT mutation culminates with a putative stress condition, even during optimal growth conditions. We further observed that the drastic reduction in the enzymatic activity of the lysine biosynthesis enzyme *L,L*-DAPAT modifies carbohydrate metabolism, reaffirming the idea of a metabolic and molecular reprogramming triggered by the DAPAT mutation, with a clear imbalance in carbon and nitrogen metabolisms (CAVALCANTI et al., 2018). Perhaps more importantly, the *L,L*-DAPAT mutation did not eliminate the capability to respond to exogenous GA, which can partially rescue the dwarf phenotype characteristic of the *dapat* mutant. Nevertheless, the application of GA_3 in *dapat* plants promoted even more severe sugar starvation symptoms at the molecular level that is most likely driven by multiple levels of regulation, shaping the metabolic changes observed in this work. Whilst the data described here provide a clear connection between lysine biosynthesis, GA metabolism, and sugar starvation features, future research is clearly required to fully elucidate the factors underlying this impaired primary metabolism phenotype observed in *dapat* mutant. It will thus be interesting in future studies to evaluate the aforementioned processes temporally and simultaneously, to dissect both the cascades that control them and the real consequence of lysine biosynthetic processes on the whole life cycle of plants.

6. REFERENCES

ANGELOVICI, R. et al. A seed high-lysine trait is negatively associated with the TCA cycle and slows down Arabidopsis seed germination. **New Phytologist**, v. 189, n. 1, p. 148–159, 2011.

ARAUJO, W. L. et al. Identification of the 2-Hydroxyglutarate and Isovaleryl-CoA Dehydrogenases as Alternative Electron Donors Linking Lysine Catabolism to the Electron Transport Chain of Arabidopsis Mitochondria. **the Plant Cell Online**, v. 22, n. 5, p. 1549–1563, 2010.

ARAÚJO, W. L. et al. Protein degradation - an alternative respiratory substrate for stressed plants. **Trends in Plant Science**, v. 16, n. 9, p. 489–498, 2011.

ARAÚJO, W. L. et al. Metabolic control and regulation of the tricarboxylic acid cycle in photosynthetic and heterotrophic plant tissues. **Plant, Cell and Environment**, v. 35, n. 1, p. 1–21, 2012.

ARRUDA, P. et al. Regulation of lysine catabolism in higher plants. **Trends in Plant Science**, v. 5, n. 8, p. 324–330, 2000.

AZEVEDO, R. A. et al. The biosynthesis and metabolism of the aspartate derived amino acids in higher plants. **Phytochemistry**, v. 46, n. 3, p. 395–419, 1997.

BARROS, J. A. S. et al. Autophagy Deficiency Compromises Alternative Pathways of Respiration following Energy Deprivation in Arabidopsis thaliana. **Plant Physiology**, v. 175, n. 1, p. 62–76, 2017.

BECKMANN, J. D.; FRERMAN, F. E. Electron-Transfer Flavoprotein-Ubiquinone Oxidoreductase from Pig Liver: Purification and Molecular, Redox, and Catalytic Properties. **Biochemistry**, v. 24, n. 15, p. 3913–3921, 1985.

BIDADI, H. et al. Effects of shoot-applied gibberellin/gibberellin-biosynthesis inhibitors on root growth and expression of gibberellin biosynthesis genes in Arabidopsis thaliana. **Plant Root**, v. 4, p. 4–11, 2010.

BRADFORD, M. A rapid and sensitive method for the quantitation of microgram quantities of protein utilizing the principle of protein-dye binding. **Analytical Biochemistry**, v. 72, n. 1–2, p. 248–254, 1976.

CAVALCANTI, J. H. F. et al. An L,L-diaminopimelate aminotransferase mutation leads to metabolic shifts and growth inhibition in Arabidopsis. **Journal of experimental botany**, v. 69, n. 22, p. 5489–5506, 2018.

CHIA, D. W. et al. Fumaric acid: an overlooked form of fixed carbon in Arabidopsis and other plant species. **Planta**, v. 211, n. 5, p. 743–751, 6 out. 2000.

DELLAPORTA, S. L.; WOOD, J.; HICKS, J. B. A plant DNA minipreparation: Version II. **Plant Molecular Biology Reporter**, v. 1, n. 4, p. 19–21, set. 1983.

ENGQVIST, M. et al. Two D-2-hydroxy-acid dehydrogenases in Arabidopsis thaliana with catalytic capacities to participate in the last reactions of the methylglyoxal and β-oxidation pathways. **Journal of Biological Chemistry**, v. 284, n. 37, p. 25026–25037, 2009.

FERNIE, A. R. Planta-2001-Fernie-Metabolites. p. 250–263, 2001.

FLEET, C. M. et al. Overexpression of AtCPS and AtKS in Arabidopsis Confers Increased ent-Kaurene Production But No Increase in Bioactive Gibberellins 1. **Plant Physiology**, v. 132, p. 830–839, 2003.

FUJIKI, Y. et al. Dark-inducible genes from Arabidopsis thaliana are associated with leaf senescence and repressed by sugars. **Physiologia Plantarum**, v. 111, n. 3, p. 345–352, 2001.

GALILI, G. The aspartate-family pathway of plants: Linking production of essential amino acids with energy and stress regulation. **Plant Signaling and Behavior**, v. 6, n. 2, p. 192–195, 2011.

GALILI, G. et al. The role of photosynthesis and amino acid metabolism in the energy status during seed development. **Frontiers in Plant Science**, v. 5, n. September, p. 1–6, 2014.

GIBON, Y. et al. A Robot-Based Platform to Measure Multiple Enzyme Activities in Arabidopsis Using a Set of Cycling Assays: Comparison of Changes of Enzyme Activities and Transcript Levels during Diurnal Cycles and in Prolonged Darkness W. [s.d.].

GIBON, Y. et al. Adjustment of diurnal starch turnover to short days: Depletion of sugar during the night leads to a temporary inhibition of carbohydrate utilization, accumulation of sugars and post-translational activation of ADP-glucose pyrophosphorylase in the followin. **Plant Journal**, v. 39, n. 6, p. 847–862, 2004.

GIBON, Y. et al. Adjustment of growth, starch turnover, protein content and central metabolism to a decrease of the carbon supply when Arabidopsis is grown in very short photoperiods. **Plant, Cell and Environment**, v. 32, n. 7, p. 859–874, 2009.

GOLLDACK, D. et al. Gibberellins and abscisic acid signal crosstalk: Living and developing under unfavorable conditions. **Plant Cell Reports**, v. 32, n. 7, p. 1007–1016, 2013.

GONZALI, S. et al. Identification of sugar-modulated genes and evidence for in vivo sugar sensing in Arabidopsis. **Journal of Plant Research**, v. 119, n. 2, p. 115–123, 7 mar. 2006.

GRAF, A. et al. Circadian control of carbohydrate availability for growth in Arabidopsis plants at night. v. 107, n. 20, 2010.

GU, L.; JONES, A. D.; LAST, R. L. Broad connections in the Arabidopsis seed metabolic network revealed by metabolite profiling of an amino acid catabolism mutant. **Plant Journal**, v. 61, n. 4, p. 579–590, 2010.

HAUVERMALE, A. L.; ARIIZUMI, T.; STEBER, C. M. Gibberellin signaling: A theme and variations on DELLA repression. **Plant Physiology**, v. 160, n. 1, p. 83–92, 2012.

HEDDEN, P. **Gibberellin Biosynthesis in Higher Plants**. [s.l: s.n.]. v. 49

HEDDEN, P.; KAMIYA, Y. GIBBERELLIN BIOSYNTHESIS: Enzymes, Genes and Their Regulation. **Annual Review of Plant Physiology and Plant Molecular Biology**, v. 48, n. 1, p. 431–460, 1997.

HEDDEN, P.; THOMAS, S. G. Gibberellin biosynthesis and its regulation. **Biochemical Journal**, v. 444, n. 1, p. 11–25, 2012.

HERNÁNDEZ-GARCÍA, J.; BRIONES-MORENO, A.; BLÁZQUEZ, M. A. Origin and evolution of gibberellin signaling and metabolism in plants. **Seminars in Cell and Developmental Biology**, n. March, p. 0–1, 2020.

HILDEBRANDT, T. M. et al. Amino Acid Catabolism in Plants. **Molecular Plant**, v. 8, n. 11, p. 1563–1579, 2015.

HISAMATSU, T. et al. The involvement of gibberellin 20-oxidase genes in phytochrome-regulated petiole elongation of Arabidopsis. **Plant Physiology**, v. 138, n. 2, p. 1106–1116, 1 jun. 2005.

HUDSON, A. O. et al. Biosynthesis of lysine in plants: Evidence for a variant of the known bacterial pathways. **Biochimica et Biophysica Acta - General Subjects**, v. 1721, n. 1–3, p. 27–36, 2005.

HUDSON, A. O. et al. An <scp>ll</scp> -Diaminopimelate Aminotransferase Defines a Novel Variant of the Lysine Biosynthesis Pathway in Plants. **Plant Physiology**, v. 140, n. 1, p. 292–301, 1 jan. 2006.

ISHIZAKI, K. The Critical Role of Arabidopsis Electron-Transfer Flavoprotein:Ubiquinone Oxidoreductase during Dark-Induced Starvation. **the Plant Cell Online**, v. 17, n. 9, p. 2587–2600, 2005.

ISHIZAKI, K. et al. The mitochondrial electron transfer flavoprotein complex is essential for survival of Arabidopsis in extended darkness. **Plant Journal**, v. 47, n. 5, p. 751–760, 2006.

IZUMI, M. et al. Autophagy contributes to nighttime energy availability for growth in Arabidopsis. **Plant Physiology**, v. 161, n. 4, p. 1682–1693, 2013.

KIRMA, M. et al. The multifaceted role of aspartate-family amino acids in plant metabolism. **Journal of Experimental Botany**, v. 63, n. 14, p. 4995–5001, 2012.

KUHLEMEIER, C.; GREEN, P. J.; CHUA, N.-H. Regulation of gene expression in higher plants. **Annual Review of Plant Physiology**, v. 38, n. 1, p. 221–257, 1987.

LAM, H. M.; HSIEH, M. H.; CORUZZI, G. **Reciprocal regulation of distinct asparagine synthetase genes by light and metabolites in Arabidopsis thalianaPlant Journal**, 1998.

LAM HON MING; PENG, S. S. Y.; CORUZZI, G. M. Metabolic regulation of the gene encoding glutamine-dependent asparagine synthetase in Arabidopsis thaliana. **Plant Physiology**, v. 106, n. 4, p. 1347–1357, 1994.

LJUNG, K.; NEMHAUSER, J. L.; PERATA, P. New mechanistic links between sugar and hormone signalling networks. **Current Opinion in Plant Biology**, v. 25, p. 130–137, 2015.

LUO, Y. et al. Involvement of the membrane-localized ubiquitin ligase ATL8 in sugar starvation response in Arabidopsis. **Plant Biotechnology**, v. 36, n. 2, p. 107–112, 25 jun. 2019.

MARTIN, D. et al. Feed-back regulation of gibberellin biosynthesis and gene expression in Pisum sativum L. **Planta**, v. 200, n. 2, out. 1996.

MARTINS, A. O. et al. Differential root and shoot responses in the metabolism of tomato plants exhibiting reduced levels of gibberellin. **Environmental and Experimental Botany**, v. 157, p. 331–343, 2019.

MURASHIGE, T.; SKOOG, F. Murashige1962Revised.Pdf. **Physiologia Plantarum**, v. 15, p. 474–497, 1962.

NUNES-NESI, A. et al. Deficiency of mitochondrial fumarase activity in tomato plants impairs photosynthesis via an effect on stomatal function. **Plant Journal**, v. 50, n. 6, p. 1093–1106, 2007.

NUNES-NESI, A. et al. The enigmatic contribution of mitochondrial function in photosynthesis. **Journal of Experimental Botany**, v. 59, n. 7, p. 1675–1684, 2008.

OLSZEWSKI, N.; SUN, T. P.; GUBLER, F. Gibberellin signaling: Biosynthesis, catabolism, and response pathways. **Plant Cell**, v. 14, n. SUPPL., p. 61–81, 2002.

PRACHAROENWATTANA, I., et al. Arabidopsis has a cytosolic fumarase required for the massive allocation of photosynthate into fumaric acid and for rapid plant growth on high nitrogen. **The Plant Journal**, v.*62, n.*5, p.785-795, 2010.

PAPARELLI, E. et al. Nighttime sugar starvation orchestrates gibberellin biosynthesis and plant growth in Arabidopsis. **Plant Cell**, v. 25, n. 10, p. 3760–3769, 2013.

PIRES, M. V. et al. The influence of alternative pathways of respiration that utilize branched-chain amino acids following water shortage in Arabidopsis. **Plant Cell and Environment**, v. 39, n. 6, p. 1304–1319, 2016.

PORRA, R. J.; THOMPSON, W. A.; KRIEDEMANN, P. E. Determination of accurate extinction coefficients and simultaneous equations for assaying chlorophylls a and b extracted with four different solvents: verification of the concentration of chlorophyll standards by atomic absorption spectroscopy. **BBA - Bioenergetics**, v. 975, n. 3, p. 384–394, 1 ago. 1989.

RADEMACHER, W. GROWTH R ETARDANTS : Effects on Gibberellin. **Annual Review of Plant Physiology & Plant Molecular Biology**, v. 51, p. 501–531, 2000.

RATE, D. N.; GREENBERG, J. T. The Arabidopsis aberrant growth and death2 mutant shows resistance to Pseudomonas syringae and reveals a role for NPR1 in suppressing hypersensitive cell death. **Plant Journal**, v. 27, n. 3, p. 203–211, 2001.

RIBEIRO, D. M. et al. Translatome and metabolome effects triggered by gibberellins during rosette growth in Arabidopsis. **Journal of Experimental Botany**, v. 63, n. 7, p. 2769–2786, 2012.

RICHARDS, D. E. et al. : A Molecular Genetic Analysis of Gibberellin Signaling. **Annual Review of Plant Physiology and Plant Molecular Biology**, v. 52, p. 67–88, 2001.

RIEU, I. et al. The gibberellin biosynthetic genes AtGA20ox1 and AtGA20ox2 act, partially

redundantly, to promote growth and development throughout the Arabidopsis life cycle. **The Plant Journal**, v. 53, n. 3, p. 488–504, 30 out. 2007.

RUZICKA, F. J.; BEINERT, H. A new iron-sulfur flavoprotein of the respiratory chain. A component of the fatty acid beta oxidation pathway. **The Journal of biological chemistry**, v. 252, n. 23, p. 8440–5, 10 dez. 1977.

SATO, T. et al. Plant Signaling & Behavior Carbon and nitrogen metabolism regulated by the ubiquitin-proteasome system. 2011.

SCHNEIDER, C. A.; RASBAND, W. S.; ELICEIRI, K. W. NIH Image to ImageJ: 25 years of image analysis. **Nature Methods**, v. 9, n. 7, p. 671–675, 2012.

SMITH, A. M.; STITT, M. Coordination of carbon supply and plant growth. **Plant, Cell & Environment**, v. 30, n. 9, p. 1126–1149, set. 2007.

SONG, J. T. Divergent Roles in Arabidopsis thaliana Development and Defense of Two Homologous Genes, ABERRANT GROWTH AND DEATH2 and AGD2-LIKE DEFENSE RESPONSE PROTEIN1, Encoding Novel Aminotransferases. **the Plant Cell Online**, v. 16, n. 2, p. 353–366, 2004.

STITT, M.; ZEEMAN, S. C. Starch turnover: Pathways, regulation and role in growth. **Current Opinion in Plant Biology**, v. 15, n. 3, p. 282–292, 2012.

SULPICE, R. et al. Starch as a major integrator in the regulation of plant growth. **Proceedings of the National Academy of Sciences of the United States of America**, v. 106, n. 25, p. 10348–53, 2009.

SUN, T. Gibberellin Metabolism, Perception and Signaling Pathways in Arabidopsis. **The Arabidopsis Book**, v. 6, p. e0103, 2008.

SZKLARCZYK, D. et al. The STRING database in 2021: Customizable protein-protein networks, and functional characterization of user-uploaded gene/measurement sets. **Nucleic Acids Research**, v. 49, n. D1, p. D605–D612, 2021.

TANIMOTO, E. Gibberellin regulation of root growth with change in galactose content of cell walls in pisum sativum. **Plant and Cell Physiology**, v. 29, n. 2, p. 269–280, 1988.

UEGUCHI-TANAKA, M. et al. Gibberellin Receptor and Its Role in Gibberellin Signaling in Plants. **Annual Review of Plant Biology**, v. 58, n. 1, p. 183–198, 2007.

UNTERGASSER, A. et al. Primer3—new capabilities and interfaces. **Nucleic Acids Research**, v. 40, n. 15, p. e115–e115, ago. 2012.

WANG, H. et al. Reference genes for normalizing transcription in diploid and tetraploid Arabidopsis. **Scientific Reports**, v. 4, 27 out. 2014.

WATANABE, N. et al. Crystal Structure of ll-Diaminopimelate Aminotransferase from Arabidopsis thaliana: A Recently Discovered Enzyme in the Biosynthesis of l-Lysine by Plants and Chlamydia. **Journal of Molecular Biology**, v. 371, n. 3, p. 685–702, 2007.

YAMAGUCHI, S. Gibberellin Metabolism and its Regulation. **Annual Review of Plant Biology**, v. 59, n. 1, p. 225–251, 2008.

YANG, Q.; ZHAO, D.; LIU, Q. Connections Between Amino Acid Metabolisms in Plants: Lysine as an Example. **Frontiers in Plant Science**, v. 11, n. June, p. 1–8, 2020.

ZHAI, Z. et al. Trehalose 6-Phosphate Positively Regulates Fatty Acid Synthesis by Stabilizing WRINKLED1. **The Plant Cell**, v. 30, n. 10, p. 2616–2627, out. 2018.

7. SUPPLEMENTARY DATA

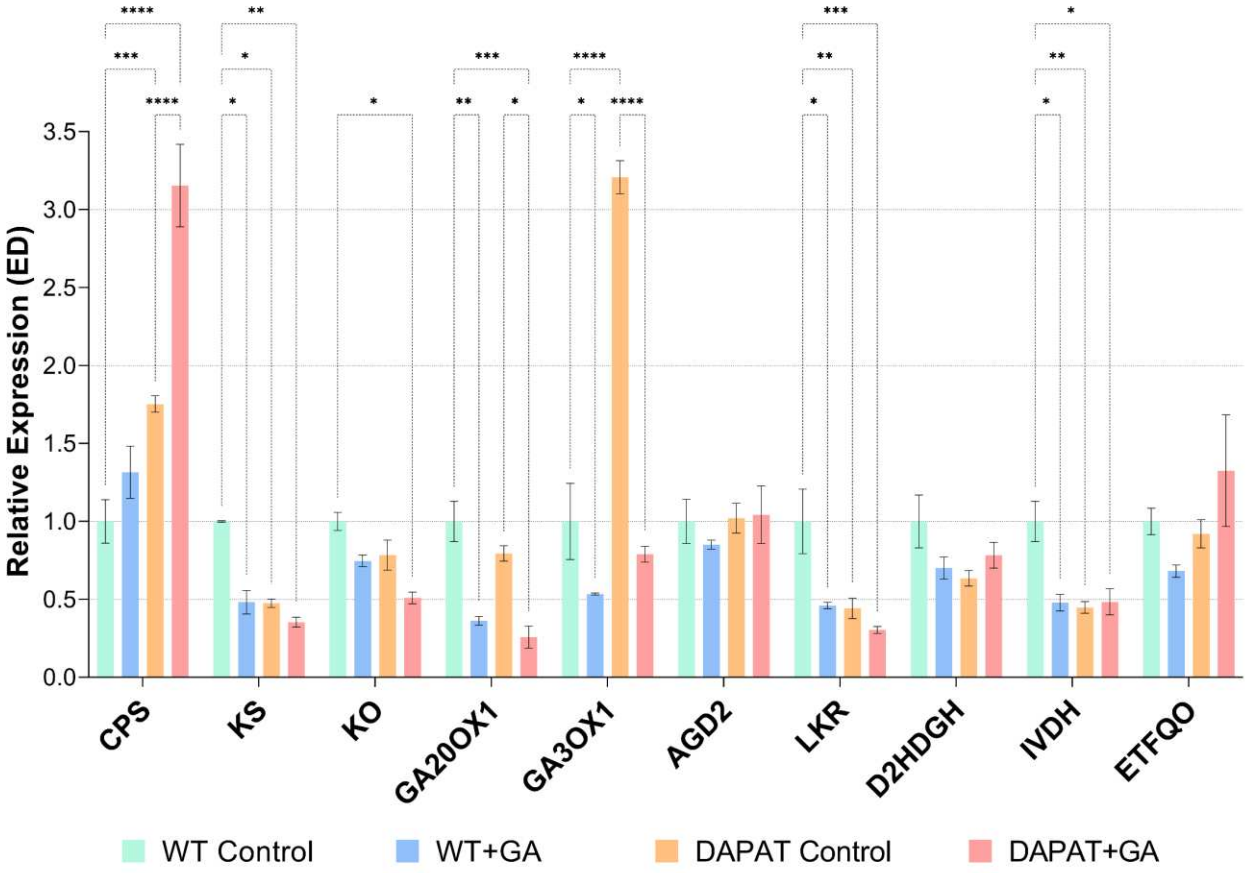

Supplementary Figure 1 – Relative expression levels of genes encoding enzymes involved GA biosynthesis and amino acids metabolism in *either Arabidopsis thaliana under* control conditions (Control) or following exogenous GA-treatment (+GA). RT-qPCR analysis of transcript levels of *CPS* gene (At4g02780), *KS* (At1g79460), *KO* (At5g25900), *GA20ox1* (At4g25420), *GA3ox1* (At1g15550), *AGD2 (*At4g33680)*, LKR/SDH (*At4g33150)*, D2HGDH (*At4g36400)*, IVDH (*At3g45300)*, ETFQO (*At2g43400). Expression levels are normalized $2^{-\Delta Ct}$ at the end of the day. Data are mean of three replicates (± SEM).

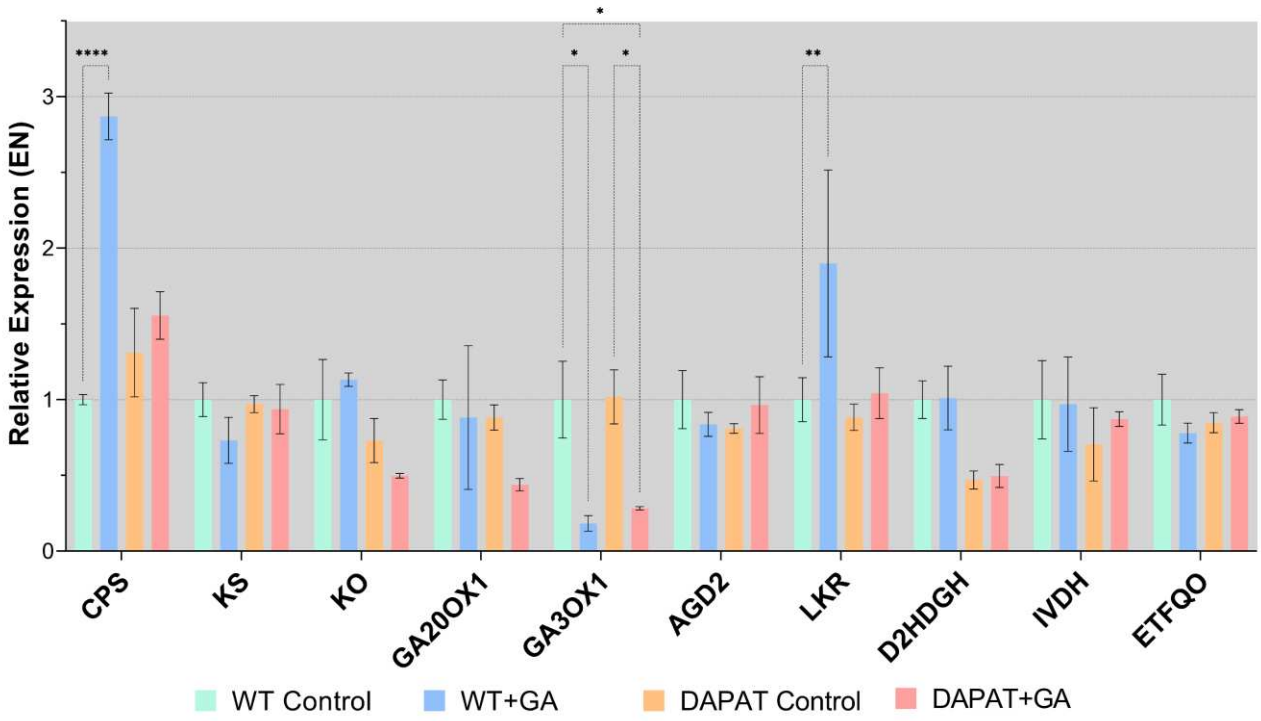

Supplementary Figure 2 – Relative expression levels of genes encoding enzymes involved GA biosynthesis and amino acids metabolism in *either Arabidopsis thaliana under* control conditions (Control) or following exogenous GA-treatment (+GA). RT-qPCR analysis of transcript levels of *CPS* gene (At4g02780), *KS* (At1g79460), *KO* (At5g25900), *GA20ox1* (At4g25420), *GA3ox1* (At1g15550), *AGD2 (*At4g33680)*, LKR/SDH (*At4g33150)*, D2HGDH (*At4g36400)*, IVDH (*At3g45300)*, ETFQO (*At2g43400). Expression levels are normalized $2^{-\Delta Ct}$ at the end of the night. Data are mean of three replicates (± SEM).